remote sensing

MDPI

Review

Twenty Years of Remote Sensing Applications Targeting Landscape Analysis and Environmental Issues in Olive Growing: A Review

Gaetano Messina and Giuseppe Modica *

Dipartimento di Agraria, Università degli Studi Mediterranea di Reggio Calabria, Località Feo di Vito, I-89122 Reggio Calabria, Italy
* Correspondence: giuseppe.modica@unirc.it

Abstract: The olive (*Olea europaea* L.) is an iconic tree linked to the birth of some of the most ancient civilizations and one of the most important cultivated tree species in the Mediterranean basin. Over the last few decades, given the high socio-economic importance of the olive sector, there has been much research involving remote sensing (RS) applications in olive growing, especially in precision agriculture. This review article is part of a review that aims to cover the past, from the 2000s onwards, and the most recent applications of remote sensing (RS) in olive growing to be able to include research and all topics related to the use of RS on olive trees. As far as the use of RS platforms such as satellites, aircraft, and unmanned aerial vehicles (UAVs) in olive growing is concerned, a review of the literature showed the presence of several works devoted to it. A brief introduction on the history of the olive tree and its distribution and cultivation around the world, together with a summary of the leading RS platforms (a good portion of which are satellites) used in olive research, anticipates the discussion of four topics about olive growing that have as their common thread positive (and non-positive) impacts on the environment: preservation of olive landscape and soil erosion, identification of olive groves, olive oil mill wastewater (OOMW) and relative environmental risks, irrigation water management and the use of RS platforms for water stress monitoring. The preservation of olive groves as an element of Mediterranean identity and strategic economic resource in agriculture depends on sustainable environmental management alongside technological advances brought by precision agriculture.

Keywords: olive landscape and land use; water stress; irrigation water management; olive oil mill wastes (OOMW); unmanned aerial vehicles (UAVs) and satellite imagery

Citation: Messina, G.; Modica, G. Twenty Years of Remote Sensing Applications Targeting Landscape Analysis and Environmental Issues in Olive Growing: A Review. *Remote Sens.* **2022**, *14*, 5430. https://doi.org/10.3390/rs14215430

Academic Editor: Raffaele Casa

Received: 2 September 2022
Accepted: 20 October 2022
Published: 28 October 2022

1. Introduction

The olive (*Olea europaea* L.) is an iconic tree linked to the birth of some of the most ancient civilizations [1–3] and one of the most important cultivated tree species in the Mediterranean basin. Moreover, the olive tree is considered one of the best biological indicators of the Mediterranean climate [1,2,4,5]. According to archaeological and genetic studies, the olive tree was probably domesticated from its wild ancestor, the oleaster (*Olea europaea* ssp. *europaea* var. *sylvestris*), about 6000 years ago in the Middle East, in an area between Turkey and Syria [1,6,7]. The olive tree as we know it today results from selective breeding aimed at obtaining varieties without thorns (present with small olives in the oleaster trees) and fruits containing more oil. The history of the olive is increasingly intertwined with that of the people who learn to use and appreciate its main product, the oil, first used only industrially for lighting and as an ointment, and then also as a food product [8]. Olive growing shows a potential diversification of its production, and its multifunctionality is demonstrated mainly by the types of products it can provide: the main ones are oil and table olives [9,10]. Olive cultivation is widespread in fifty-eight countries on five continents. The consumption of its products extends to 179 countries, thus showing an

extremely localized production against a dispersed demand in the international context [9]. Today, olive crops cover more than 12 million hectares [11] globally. Olive growing is roughly limited by 30° to 45° parallels [12]. The primary producers of olives are Spain, Italy, Greece, and Portugal, followed by other Mediterranean countries such as Tunisia, Morocco, Algeria, Egypt, and Turkey [11]. Among emerging producer countries, Argentina, Peru, Chile, and Australia are particularly noteworthy [11] (Figure 1), where super-intensive olive groves, irrigated and highly mechanized, represent the majority of newly cultivated areas [13]. Over the last few decades, given the high socio-economic importance of the olive sector over the last few decades, there has been much research involving Remote Sensing (RS) applications in olive growing, especially in precision agriculture (PA). As far as the use of RS platforms such as satellites, aircraft, and unmanned aerial vehicles (UAVs) in olive growing is concerned, a review of the literature showed the presence of several works devoted to it.

On the one hand, the increasing availability of data and the possibility of using increasingly higher-resolution imagery helped make satellite the platform commonly associated with RS in the first decade of the 2000s. On the other hand, technological advances have affected UAVs over the last decade, making them a potential game-changer in PA applications [14], mounting sensors with centimeter spatial resolution and more independent of climatic variables [15]. In addition, UAVs have the unique feature of being able to mount several types of sensors simultaneously [16].

RS has the potential to provide biodiversity information at the site, landscape, continental, and global spatial scale and offers itself as an inexpensive means of obtaining comprehensive spatial coverage of updatable environmental information [17–20]. The spatial resolution image, increasing as technology advances in this field, provides data on scales of individual tree canopies over a wide area. RS sensors allow the detection of species or single trees and their density and land covers due to high spatial resolution, which increases the accuracy of the data [21–23]. The potentialities of the application of RS in olive growing have concerned so far several mapping and monitoring issues, such as the identification of olive-cultivated areas and tree counting [24,25], evaluation of the effects of pruning strategies [26,27], plant phenotyping [28], as well as the relationship between plant structure and growth with irrigation and water stress [29], and yield estimation [30–32]. In addition to purely agronomic issues, RS data helps monitor the evolution of pathogens and phytophagous infections and, on a larger scale, the olive landscape characteristics [33]. What is also critical for their environmental issues is managing wastewater produced by the olive oil industry. Olive oil extraction generates enormous waste that significantly impacts terrestrial and aquatic environments [34]. In this framework, the role of RS platforms can be to monitor this source of underground pollution related to olive oil waste disposal areas, which is considered a major environmental problem in Mediterranean countries [35].

This review aims to cover the past, from the 2000s onwards, and the most recent applications of RS in olive growing, focusing on preserving the olive landscape and addressing environmental issues. A review of RS applications focusing on detecting and counting trees, phenotyping, yielding, detecting olive diseases, and managing pests in the framework of PA is reported in Messina and Modica [36]. The structure of the first part of this review is the following: Section 2 contains brief mentions of RS platforms and sensors, mainly satellites and UAVs, used in research focused on olive growing from the early 2000s until now; Section 3 deals with the preservation of olive landscape and soil erosion; Section 4 regards RS applications aiming to identify and mapping olive groves; Section 5 is focused on monitoring and management of olive oil mill wastewater (OOMW) and relative environmental risks; Section 6 concerns irrigation water management and the use of RS platforms for water stress monitoring; finally, Section 7 contains discussions and conclusions about the present—as well as future—challenges in the presented framework.

Figure 2 shows that of the 41 researches considered, most were published in the second decade, from 2011 onward, while just over a quarter were published earlier. The sources

for the search of works reviewed were the following databases: Scopus (Elsevier), Google Scholar, and Web of Science (Clarivate Analytics).

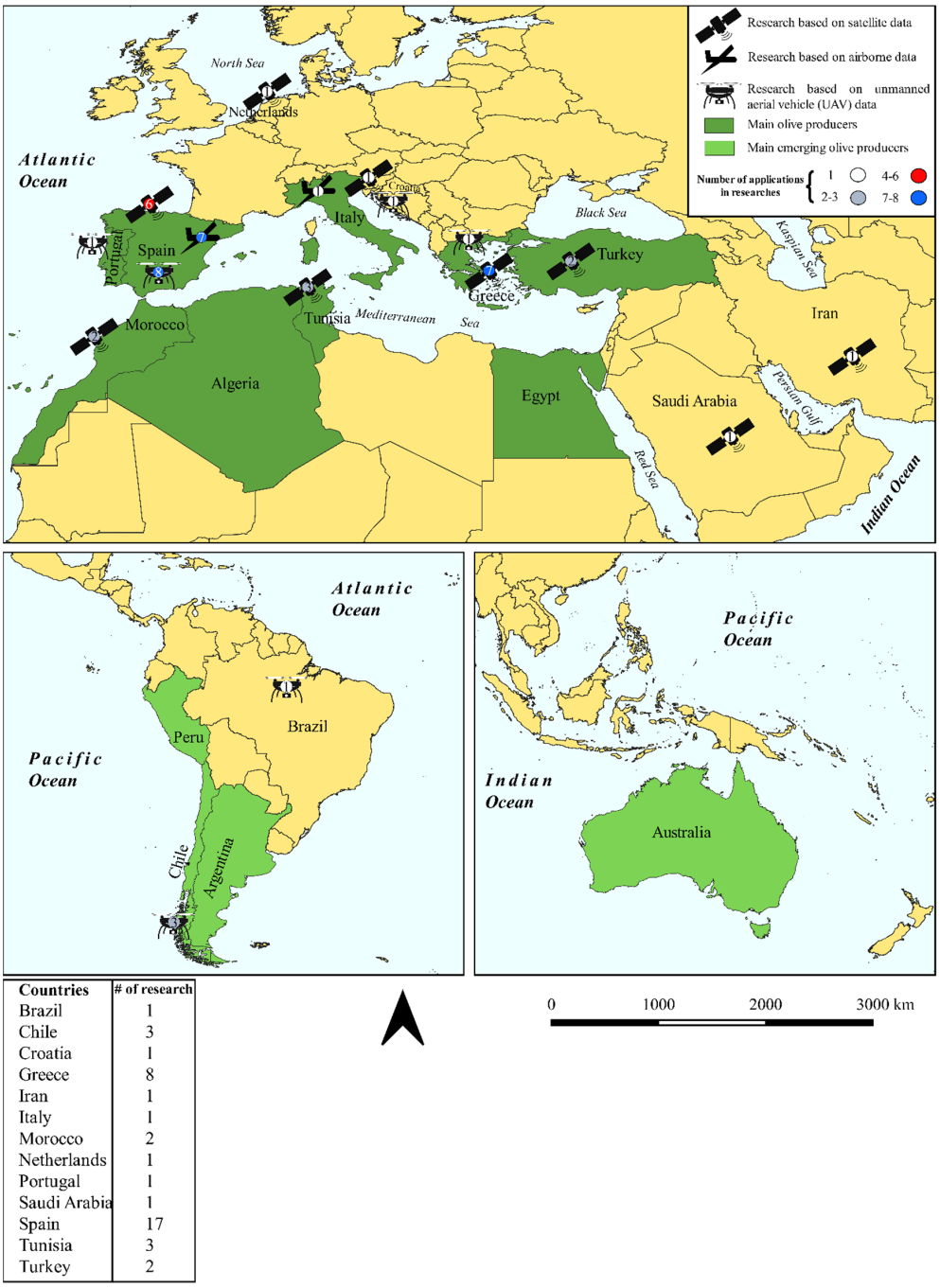

Countries	# of research
Brazil	1
Chile	3
Croatia	1
Greece	8
Iran	1
Italy	1
Morocco	2
Netherlands	1
Portugal	1
Saudi Arabia	1
Spain	17
Tunisia	3
Turkey	2

Figure 1. Map showing a comprehensive view of remote sensing (RS) applications distribution, according to the distribution of research study sites in the countries reported in the analyzed papers and the worldwide geographical distribution of olive cultivation. The main olive-producer countries are highlighted in dark green, while the main emerging-producer countries are highlighted in light green. The symbols of different color (shown in the upper right) distinguish the type of remote sensing platform (satellite, airborne, or unmanned aerial vehicle) used in the research and the number of research performed from 2000 to the end of March 2022. The table at the bottom left shows the number of remote sensing researches in olive growing carried out in each country. Important to consider that some researches include more than one RS platform.

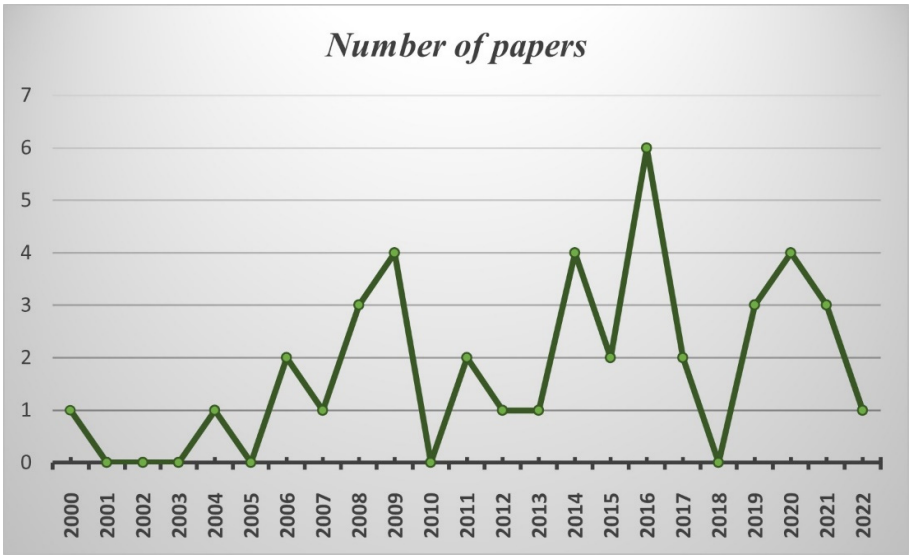

Figure 2. The trend of published articles based on publication year. The sources for the search of works reviewed were the following databases: Scopus (Elsevier), Google Scholar, and Web of Science (Clarivate Analytics). The x-axis shows the years of the period under consideration, while the y-axis shows the number of searches carried out. The researches considered are those carried out from the beginning of the year 2000 until the end of March 2022.

VOSviewer 1.6.18 software was used to perform cluster analysis on titles and abstracts (the choice is due to the lack of keywords in some of the works considered), having a frequency of at least six, and three categories were obtained (Figure 3). A temporal analysis of the period under consideration (beginning of 2000—end of March 2022) was performed. However, the software detected significant occurrences only from 2012. According to the content of words occurrence, three clusters were obtained, and in line with what is covered in this review, the most common were "environmental science", "remote sensing", and "NDVI". "Environmental science" encapsulates well the content of this review focused on the analysis of research that has included applications of RS in olive growing aimed at the conservation of the olive landscape, its monitoring, the management of irrigation resources, and environmental issues arising from the olive industry. Occurrences involving the term can be traced back to the last five years. Noteworthy are the terms "transpiration", "water content", "water", and "hydrology" inherent in both the problem of soil erosion, covered in Section 3, and irrigation and water resource preservation, covered in Section 6. As for the term "NDVI", the most widely used of indices with the largest number of researches in which it was used, and "vegetation indices", we have indicated in Table 1 the main indices used in the researches analyzed.

Table 1. The main vegetation indices (VIs) used in remote sensing research in olive growing.

Vegetation Index (VI)	Acronym	Equation	Research
Blue Normalized difference vegetation index [37]	BNDVI	$\frac{(NIR-Blue)}{(NIR+Blue)}$	[38]
Difference Vegetation Index [39]	DVI	$NIR - R$	[38,40–43]
Enhanced Vegetation Index [44]	EVI	$G \times \frac{(NIR - Red)}{(NIR + CRed - CBlue + L)}$	[40,41]
Greenness index	GI	R554/R677 *	[45]
Green Normalized Vegetation Index [46]	GNDVI	$\frac{(NIR-Green)}{(NIR+Green)}$	[38,40,47,48]
Green Ratio Vegetation Index [49]	GRVI	$\frac{NIR}{Green}$	[42]
Inverse Ratio Vegetation Index [39]	IRVI	$\frac{Red}{NIR}$	[38,42,43]

Table 1. *Cont.*

Vegetation Index (VI)	Acronym	Equation	Research
Modified chlorophyll absorption in reflectance index [50]	$MCARI_1$	$1.2[2.5(NIR - Red) - 1.3(NIR - Green)]$	[45]
Modified chlorophyll absorption in reflectance index [50]	$MCARI_2$	$\frac{1.5(2.5(NIR-Red)-1.3(NIR-Green))}{\sqrt{(2NIR+1)^2-(6NIR-5\sqrt{Red})-0.5}}$	[45]
Modified Simple Ratio [51]	MSR	$\frac{(NIR/Red-1)}{\sqrt{NIR/Red+1}}$	[40,47]
Modified Soil Adjusted Vegetation Index [52]	MSAVI	$[2\ NIR + 1 - [(2\ NIR + 1)^2 - 8(NIR - Red)]^{0.5}]/2$	[38,40,41,45,47]
Modified triangular vegetation index [50]	$MTVI_1$	$1.2 \times [1.2 \times (NIR - Green) - 2.5 \times (Red - Green)]$	[45]
Modified triangular vegetation index [50]	$MTVI_2$	$\frac{1.5(1.2(NIR-Green)-2.5(Red-Green))}{\sqrt{(2NIR+1)^2-(6NIR-5Red)-0.5}}$	[45]
Normalized difference green/red index [53]	NGRDI	$\frac{(Green-Red)}{(Green+Red)}$	[42]
Normalized Difference Red Edge Index [54]	NDRE	$\frac{(NIR-Red\ Edge)}{(NIR+Red\ Edge)}$	[48]
Normalized Ratio Vegetation Index [55]	NRVI	$(RVI - 1)/(RVI + 1)$	[42,43]
Normalized Difference Vegetation Index [56]]	NDVI	$\frac{(NIR-Red)}{(NIR+Red)}$	[38,40,42,43,45, 47,48,57–66]
Optimized Soil Adjusted Vegetation Index [67]	OSAVI	$1.16\ \frac{(NIR - Red)}{(NIR + Red + 0.16)}$	[40,41,43,45,47]
Renormalized Difference Vegetation Index [68]	RDVI	$\frac{(NIR-Red)}{\sqrt{(NIR+Red)}}$	[41]
Simple Ratio [69]	SR	$\frac{NIR}{Red}$	[40–42,47]
Soil Adjuted Vegetation Index [70]	SAVI	$\frac{(NIR - Red)}{(NIR + Red + L)} \times (1 + L)$	[40,41,47,71]
Soil and Atmospherically Resistant Vegetation Index [72]	SARVI	$(1 + L)(NIR - Red_{rb})/(NIR + Red_{rb} + L)$	[38]
Transformed Soil Adjusted Vegetation Index [55]	TSAVI	$\frac{[a(NIR-aRed-Blue)]}{[Red+aNIR-ab)]}$	[38]
Transformed Vegetation Index [73]	TVI	$(NDVI + 0.5)^{0.5}$	[43]
Vogelmann Red Edge Index [74]	VREI	$\frac{NIR}{Red\ Edge}$	[42]

* R = reflectance. NIR = near-infrared. L = soil adjustment factor ranging from 0 to 1.

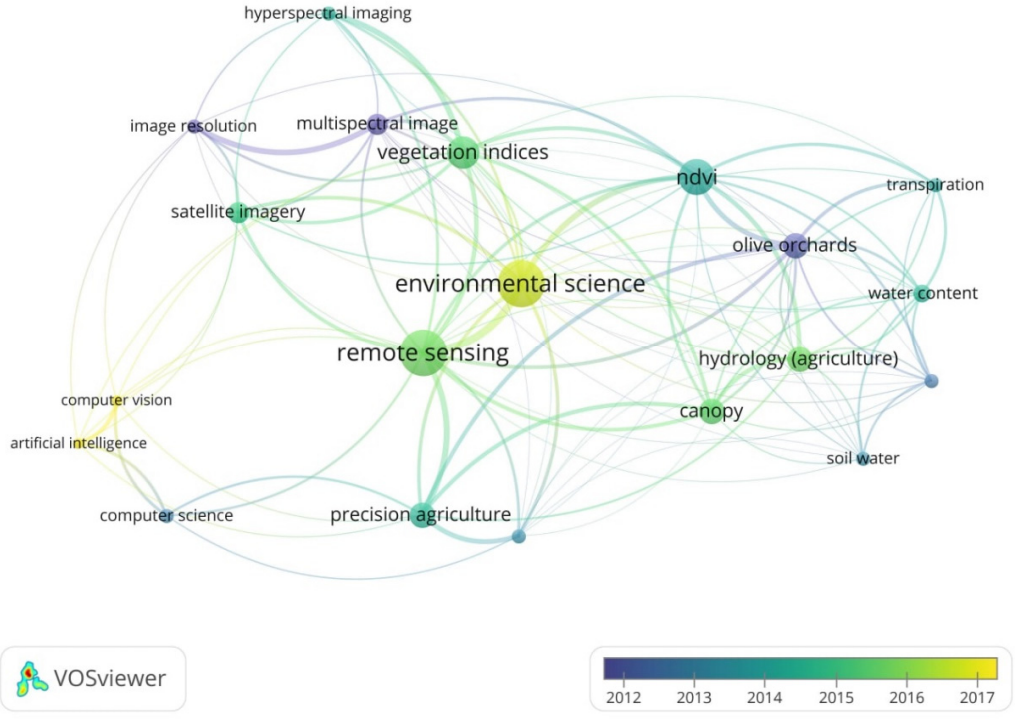

Figure 3. Keywords occurrence and clustering by VOSviewer 1.6.18. Colors indicate the year in which each title and word contained in the abstracts were used more. Lines represent co-occurrence link strength among terms.

2. Remote Sensing Platforms and Sensors

2.1. Satellites

Initially, RS relied on aircraft-mounted photographic instruments to capture Earth features taking imagery flying within a height of 10 km above the ground [75]. Aerial platforms proper include fixed-wing aircraft, helicopters, balloons, dirigibles, rockets, kites, parachutes, and in recent times military-operated drones from which drones are derived for civilian use, the UAVs [14]. Before the advent of the well-known UAVs, several satellites regularly provided data covering a wide spectral range, using both active and passive sensors [76], acquiring data from different orbits and at different spatial and temporal resolutions [77]. Satellites have been used for RS imagery in agriculture since the early 1970s [78], using a sensor mounted on the Landsat 1 (also known as the Earth Resources Technology Satellite—ERTS), launched in 1972. Landsat 1 was followed by its improved versions (from Landsat 2 to 9, the latter launched on 27 September 2021) and equipped with sensors with increasing higher performance in terms of bandwidth, radiometric and spatial resolution. The satellite "evolved" from the initial 4 bands (green, red, and two near-infrared—NIR-bands) to the current 11 bands (coastal aerosol, blue, green, red, NIR, short-wave infrared (SWIR 1), and SWIR 2, panchromatic (PAN), cirrus and two thermal bands). The spatial resolution increased from a maximum of 80 m of Landsat 1 to 30 and 15 m of the multispectral (MS) and panchromatic bands, respectively, of Landsat 7, 8, and 9 [79]. The Landsat historical archive was made freely available in 2008 (for Landsat 7) and 2009 (for all archived Landsat scenes) [80]. The benefits of this decision can be seen in the use of Landsat imagery in the multi-temporal monitoring of changes in land uses, considering an increased awareness of the implications of rapid land use and cover changes occurring in the landscape [75,81]. In olive growing-related research, Landsat imagery was primarily used in land-use mapping and monitoring of sites of OOMW disposal areas [40,47,71,82–85]. Images with lower resolution than Landsat are those produced by Terra satellite's sensor, Moderate Resolution Imaging Spectro-Radiometer (MODIS), acquiring at 250–500 m resolution data related to surface reflectance and land surface temperature (LST) and emissivity, land cover/change, vegetation indices (VIs), thermal anomalies and fire data, leaf area index (LAI), the fraction of photosynthetically active radiation (PAR), net primary vegetation production, etc. [80]. Another Terra sensor, Advanced Spaceborne Thermal Emission and Reflection Radiometer (ASTER), equipped with 15 bands and including some of them with 15 m resolution, is suitable for the measurement of soil properties, vegetation and crop monitoring, land temperatures, and generation of digital elevation models (DEMs) [86]. In the framework of olive growing RS research, MODIS and ASTER imagery was used to monitor canopies' temperature, yield predicting, water stress, and irrigation management [30,31,45,87,88].

Following the period of "preeminence" of the Landsat system, several private consortia developed, between the late 90s and early 2000s, a new generation of satellites with a high spatial resolution (between 0.5 and 4 m) to open up new markets for satellite imagery [86]. Until then, satellite imagery has proven cost-effective compared to aerial photography previously used for land use classification over large regions [89]. However, coarse spatio-temporal resolution satellite imagery is not entirely adequate for PA applications. Among the first high-resolution systems launched and operated by private companies were IKONOS and Quickbird. The IKONOS satellite system was launched in September 1999. It was the first commercial satellite providing submeter imagery with 0.80 m resolution, using a PAN band or combined with other bands to produce pansharpened MS imagery. Quickbird was launched in October 2001 and provided imagery at 0.60 m resolution, exploiting pansharpened MS imagery and 2.4 m using MS bands [90]. With the highest spatial resolution available, pansharpening routines are widely used to optimize the spectral and spatial resolution of MS bands [91]. The availability of the first images provided by these two satellites allowed researchers to address issues that previously could not be studied from space or on the ground, such as individual mapping canopies, as shown in research focused on detecting and counting olive trees [92–95].

For some years, IKONOS and Quickbird satellites provided the highest resolution satellite imagery available to the public before the advent of WorldView satellites (2007–2009) and GeoEye-1 (in 2008) [80]. These satellites provide PAN imagery at a resolution from 30 to 50 cm and MS imagery at less than 2 m [86]. GeoEye, WorldView-2, and -3 images were used to detect OOMW disposal areas [57] and monitor olive trees' health status using VIs [96,97]. Another important commercial source of data, albeit limitedly used RS research in olive growing [41,98,99], is the Planetscope constellation launched in the middle of the past decade. PlanetScope constellation is composed of many small nano-satellites, 3U CubeSats, also called "Doves" and equipped with MS sensors providing up to 3 m spatial resolution with a one-day revisiting time [100,101].

While commercial satellites are worthy of consideration, the Sentinel constellations operated through the Copernicus program proposed by the European Union (EU) and the European Space Agency (ESA) today play a significant role. The Copernicus program includes Sentinel-1′s constellation, with two satellites using radar C-band, and Sentinel-2′s constellation, comprising two MS satellites, providing image resolution between 10 and 60 m. Sentinel images are particularly suitable both for the monitoring of environmental risks and for the needs of the agricultural and academic communities considering the free availability of data to users together with its spatial and temporal resolution [102–105]. Sentinel images have proven useful in monitoring the health of olive groves by detecting water stress symptoms in olive trees caused by *Verticillium dahliae Kleb.* [106] and temporal variations in the olive canopy associated with Xylella fastidiosa's symptoms [107,108]. In addition to Sentinel-1 radar images, Radarsat 2, COSMO-SkyMed, and TerraSAR-X satellites were exploited to map olive groves and characterize canopy biophysical parameters [109–111]. The main characteristics of satellites used in olive-growing applications (from 2000 to date) are summarized in Table 2.

Table 2. The main characteristics of satellites used in olive growing applications.

Satellite and Sensors	Spectral Bands	Ground Sample Distance (GSD)	Temporal Resolution	Temporal Cover Age
COSMO-SkyMed	X-band SAR	2.5 m	5 days	2007–present
GeoEye 1	PAN-VIS-NIR	0.4 m PAN 1.6 m MS	2–5 days	2008–present
IKONOS	PAN-VIS-NIR	0.8 m PAN 3.6 m MS	3 days MS 12 days PAN	1999–2015
Landsat 5 Thematic Mapper (TM)	VIS-NIR	30 m	16 days	1984–2012
Landsat 8	PAN-VIS-NIR	15 m PAN 30 m MS	16 days	2013–present
PlanetScope	VIS-NIR	3.6 m	1 day	2017–present
Pleiades	PAN-VIS-NIR	0.5 m PAN 2 m MS	1 day	2011–present
Quickbird	PAN-VIS-NIR	0.6 m PAN 2.5 m MS	3 days	2001–2015
Radarsat 2	C-band SAR	3 to 100 m	3 days	2007–present
Sentinel-1	C-band SAR	5 m × 20 m	1–3 days	2014–present
Sentinel-2	VIS-NIR	10 m	5 days	2015–present
SPOT 5	PAN-VIS-NIR	2.5–5 m PAN 10 m MS	2–3 days	2002–2015
SPOT 6	PAN-VIS-NIR	1.5 m PAN 6 m MS	1 day	2010–present

Table 2. *Cont.*

Satellite and Sensors	Spectral Bands	Ground Sample Distance (GSD)	Temporal Resolution	Temporal Cover Age
Terra (EOS AM-1): Advanced Space-Borne Thermal Emission and Reflection Radiometer (ASTER)	VIS-NIR	15 m	4–16 days	1999–present
Terra (EOS AM-1): Moderate-resolution Imaging Spectroradiometer (MODIS)	VIS-NIR	250–500 m	2 days	1999–present
TerraSAR-X	X-band SAR	3 m	3 days	2007–present
WorldView-2	PAN-VIS-NIR	0.46 m PAN 1.84 m MS	1 day	2009–present
WorldView-3	PAN-VIS-NIR	0.31 m PAN 1.24 m MS	1 day	2014–present

VIS = visible. PAN = panchromatic. NIR = near-infrared. SAR = Synthetic Aperture Radar. MS = multispectral.

2.2. Unmanned Aerial Vehicles (UAVs)

UAVs are widely used in geomatics for data acquisition in research and operational fields, among which security and surveillance, civil infrastructure inspection, monitoring of archaeological sites, environmental monitoring, and applications in agriculture and forestry [112–117]. In agricultural applications, UAVs' use registered its spread over the last decade [16].

UAVs are generally equipped with miniaturized and lower-cost versions than satellite sensors. They include RGB, MS, thermal, hyperspectral cameras, and light-weight LiDAR (light detection and ranging) sensors [118]. RGB sensors, on which many RS applications in agriculture are based [119], were used, as shown in much olive-related research, for tree canopy detection and tree counting [24,32,120–122], characterization of tree dimension parameters [27,123–128], and health monitoring [129]. These are relatively low-cost, high-resolution sensors but may be inadequate if not coupled with other types of sensors [112]. An alternative involves modifying RGB sensors to capture images on bands such as Red Edge and NIR, avoiding the higher costs of purchasing MS cameras [119]. MS cameras being able to operate on other bands, such as Red Edge and NIR, can be exploited for monitoring plant physiological status by detecting drought and heat stress, the health status in general, nutrient content, and plant biomass [48,130–135]. Multiple bands allow more VIs to be exploited to highlight vegetation's vigor and other vegetation properties [136] (Table 1). In addition, MS UAV imagery is used for phenotyping; detecting olive trees based on pixel or object-based image analysis (OBIA); assessing olive tree parameters such as height, diameter, and volume [25,28,29,123,127,137,138]; and monitoring them in terms of spectral behavior.

Thermal UAV cameras provide data of great agronomic relevance considering the absence of high-resolution satellite thermal sensors. Thermal sensors capture information about the temperature of objects by generating images that display them based on their temperature, not on their visible properties [119]. Therefore thermal RS, when used on the vegetation, allows for identifying the leaf surface's thermal alterations due to physiological changes induced by water stress [112]. Several researches focused on the field characterization of water stress in olive groves [139–143], and a few [144,145] correlated olive canopy temperature to the water stress symptoms to detect infected plants by Verticillium Wilt.

Hyperspectral sensors capture data in hundreds of bands providing high volumes of information in agriculture and forestry [146,147]. However, the use of these sensors mounted on UAVs is affected by some limitations: higher spectral resolution but lower spatial resolution if compared, for example, to RGB sensors; read spectral ranges halved when compared to aircraft-mounted sensors due to weight limitations; higher cost [118]. In addition, hyperspectral sensors, similarly to and more so than MS sensors, may require

more complex data pre-processing methods to extract information [119]. The difficulties linked to UAV hyperspectral use can explain the lack of much olive-related work [148].

LiDAR, mainly used for terrestrial scanning, has been used for aerial scanning since 1994, when commercial systems became available. LiDAR is an active RS system emitting pulses whose return to the sensor after being reflected by an "object" of the terrestrial surface is measured by calculating the time elapsed between the emission of the energy pulse and its return [86]. From this information, it is obtained a cloud of points with X, Y, and Z coordinates that corresponds to the impacts of the initial pulse energy on the Earth's surface objects, thus making it possible to reconstruct the structure of trees with high precision digitally [26,149,150]. LiDAR sensors are known to be very accurate for acquiring geometric data, such as those referring to tree canopies, many of which are carried out in forestry [151,152]. 3D models obtained from LiDAR surveys can also be helpful in agriculture, with applications similar to those used in forest areas. As the geometric characteristics of trees are directly related to tree growth and productivity, they can be important indicators for estimating growth, yield prediction, and water consumption [153]. However, even those with a relatively low cost are still more expensive than RGB cameras and require higher payloads (up to a few kilograms) [119,154]. For these reasons, the LiDAR system is not as readily accessible as other UAV-based photogrammetric mapping systems [118].

3. Preservation of the Olive Landscape and Soil Erosion

The olive grove can be considered an essential and historical component of the Mediterranean landscape mosaic, especially in Italy, Spain, and Greece [155–157]. The landscape has the constant trait in this species, while other characters are given by different environmental and cultural expressions such as climate, land geomorphology, and cultivation techniques. The climate is a relatively limiting factor considering the spread in recent decades of olive growing even in areas far from those "historical" cultivation [158]. Just think of the growing importance that olive cultivation is acquiring in the countries of South America (Argentina, Chile) and Australia [159]. As for the geomorphology, this is closely linked to both the olive groves localization and the cultivation techniques adopted, and examples of this are the traditional terraced olive groves typical of hilly-mountainous and marginal areas of Greece's and Italy's regions, conversely, contrasted by location, planting, and management to the super-intensive olive groves in Spain (or Australia) spread in recent decades [160]. The protection of the cultivated landscape, specifically that of the olive tree, must be pursued by complying with opposing requirements: opportunity for protection through conservation (even with the introduction of compensatory mechanisms) or freedom to organize the factors of production by appropriately modifying the productive assets and, inevitably, landscape [161]. For example, in opposition to the advancement of intensive olive growing in some areas, in others, the olive landscape's detriment is caused by urbanization's effects on agricultural land [157]. It is often overlooked that olive represents a typical crop with mixed urban-rural settlements, which provides environmental services and biodiversity conservation and represents an integral part of periurban landscapes while also supporting rural economies and tourism development [3]. The adverse effects of the urban sprawl on agricultural land were covered by Doygun [162], which quantified the loss of agricultural land, and olive land cover in particular, in a location in Turkey, from 1985, using aerial imagery, to 2006, using IKONOS' image (panchromatic), and Quickbird image (pansharpened). Three specific periods were analyzed and compared (1985–2000, 2000–2004, and 2004–2006), starting by superimposing the olive groves digitized in the 1985 aerial photographs on 2000 urban area images. The data obtained showed a loss of 25% of the area initially occupied by olive groves due to a progressive abandonment of agricultural practices in favor of new residential building construction.

One challenge of RS is to effectively assess the impact of agriculture in risk situations concerning soil erosion and environmental conservation [163]. Soil erosion represents one of the principal environmental issues associated with olive growing in Mediterranean countries, mainly in hilly areas characterized by more or less accentuated slopes [164,165].

The evolution of soil erosion in olive groves finds in its causes both their expansion and changes in soil management techniques [166]. Soil erosion can cause several negative environmental impacts, including a reduction in production, risk of desertification, and run-off with soil transport, fertilizer residues, and herbicides into water bodies [166]. Soil erosion depends on the combination of soil characteristics, slope, rainfall patterns, and the use of inappropriate agricultural practices [167]. Mechanical tillage is still the most widely used practice for soil management as it improves not only the infiltration capacity but also the distribution of water in the soil profile and contributes to the burial of fertilizers, the prevention of fires, and the removal of weeds [168–170]. However, the continued use of this practice, in the long run, can cause opposite and harmful effects on soil destructuring, reduction of water infiltration rate, reduction of water availability in the rhizosphere, and soil compaction with consequent loss of nutrients and organic matter depriving it of protection from torrential rains [42,167,171]. Cover crops shield soil from the driving rain while increasing infiltration and reducing surface sealing [172–174].

Furthermore, vegetation cover promotes more bacterial diversity, which can be considered a biological indicator of soil quality [175]. As highlighted by Lima-Cueto et al. [42], the role of vegetation cover is acknowledged in the cross-compliance system of the EU Common Agricultural Policy (CAP) (Regulation No. 1306/2013). Lima-Cueto et al. [42] exploited RS for quantifying cover crops (CC) in olive groves where CC contributes to improving soil fertility and water retention while reducing erosion risk. For this purpose, the authors tested several VIs, chosen from those contained in their formula, the bands Green, Red, Red Edge, and NIR, to verify their capacity to quantify the density of cover crops in olive groves using UAV imagery. Results showed that the Inverse Ratio Vegetation Index (IRVI, given by the ratio of Red to NIR) [39] was the most sensitive for quantifying CC density at intervals of 10–25%. Given its impact on soil conservation in sloping farmlands, Lima et al. [163] used UAV MS data and DEMs to map differences in tillage using OBIA classification techniques. Authors automatically classified tillage furrows and computed their main direction testing this procedure on twenty olive groves characterized by a wide range of tree sizes, soil tones, plot shapes, and soil slopes.

Karydas et al. [137] investigated soil erosion risk mapped in Creta (Greece) caused by the intensification of olive growing. As in other regions of the Mediterranean, long periods of drought followed by heavy rainfall favor erosion on steep slopes and with shallow and fragile soils. In this regard, the use of terraces and the presence of rural roads perpendicular to the direction of the slope helps to divide the length of the slope and slow down the runoff process, improving water penetration. Erosion is related to the speed with which water passes or infiltrates the soil and the generation of runoff, the leading cause of soil loss [165]. The authors used Quickbird imagery, a DEM, a geologic map, and rainfall data collected by two meteorological stations. The research aimed to quantify the supporting practice factor (P) in the spatial domain and its incorporation into the Revised Universal Soil Loss Equation (RUSLE) formula. RUSLE is a revised version of the model-based method Universal Soil Loss Equation (USLE) used for quantifying the risk of soil erosion [176]. P factor depends on the mapping landscape's features indicative of existing support measures (terraces) or conditions that prevent soil erosion (rural roads and paths). P factor was quantified using visual photointerpretation for an overall image interpretation and object-oriented image analysis for semi-automatically mapping terraces and rural roads. A soil erosion risk map was produced, attributing differentiated values to the P factor.

Terraces perform an essential service by leveling the soil surface and stabilizing slopes, resulting in better water infiltration and reduced erosion risk. In addition, terraces increase landscape diversity and function as habitats and biodiversity corridors [177]. Conversely, the abandonment of terraces may cause an aggravation of the eroding process [178–180]. Considering the aspects mentioned so far, Diaz-Varela et al. [143] proposed a low-cost methodology for automatically classifying agricultural terraces (with permanent crops such as olive trees) using high-resolution imagery acquired by a low-cost UAV equipped with non-metric cameras. In the context of CAP monitoring, these objectives address the need to

develop reliable and repeatable methods for automatically classifying landscape elements that perform an ecosystem service. The UAV imagery was acquired and pre-processed without ground control points for reducing flight planning costs and user interaction. The classification of terraces and no-terraces was based only on the spectral and elevation data derived from imagery and exploiting 3D photo-reconstruction methods.

Fernández et al. [181] used UAVs high-resolution imagery to analyze the evolution of a landslide affecting olive groves in Southern Spain. The proposed method allows a monitoring analysis by calculating differential Digital Surface Models (DSMs) to measure vertical displacements and identify depletion and accumulation areas inside the landslide. DSMs of different epochs were compared to monitor landslides to reach this objective: head and depletion area, primary and secondary scarp, body, toe, and accumulation area. Moreover, the estimation of vertical displacements in areas not covered by vegetation was performed. This work proved that UAVs could estimate vertical and horizontal landslide displacement changes based on DSM and Digital Terrain Model (DTM). Both models and orthophotos at different epochs were obtained from UAV surveys using a methodology based on conventional photogrammetry and Structure from Motion (SfM) techniques. The results allowed the characterization of the slope movement flow rate and some morphological features (crown, scarps, head, lateral limits, tension cracks, foot, etc.) on a hillslope of hectometric dimensions.

Part of the ecosystem functions of olive groves, especially traditional ones, is the critical contribution to animal and plant biodiversity even when they are present in areas dominated by other land uses, such as arable land and forests where, among other things, olive groves can also serve as firebreaks [167]. In particular, the biological activity and biodiversity are generally higher in undisturbed olive groves semi-abandoned or those managed according to modern techniques of conservation agriculture [182]. Tscheulin et al. [85] highlighted the olive tree's function in preserving biodiversity in Mediterranean environments. The authors analyzed the influence of the surrounding landscape, in particular olive groves, on the presence of three size groups of bees. Depending on the size of the bees and the distance they can cover, the use of resources such as pollen occurs on different spatial scales. The landscape around the study area was assessed using thematic maps based on the satellite image Landsat 5 and classifying land according to eight land cover categories. Among these, the olive grove class positively impacted the abundance of bees.

Table 3 shows the researches in RS in olive growing dealing with the preservation of the olive landscape and soil erosion.

Table 3. References dealing with the preservation of the olive landscape and soil erosion.

Reference	Platform	Sensor Type Used	Aim of the Study
[59]	UAV	CIR Panasonic Lumix DMC-GF1 (MS)	Identification of agricultural terraces
[183]	Satellite WorldView-3 UAV DJI Matrice 600 PRO	RGB Sony Alpha A7RII DSLR camera	Evaluating the vertical accuracy of WorldView-3 derived DSMs for application over olive groves
[162]	Satellites IKONOS—Quickbird Aircraft	PAN	Loss of land
[181]	UAVs Falcon 8 Asctec	Sony Nex 5N (RGB)	Landslide evolution
	Aircraft FV-8 Atyges	Canon G12 (RGB)	
[62]	Satellite Quickbird	PAN-MS	Soil erosion risk
[42]	UAV Parrot Bluegrass	Sequoia Parrot (MS)	Quantify the vegetation ground cover
[163]	UAV DJI Phantom 4 Pro	Sequoia Parrot (MS)	Mapping tillage direction
[85]	Satellite Landsat 5	MS	Influence of olive groves on the diversity of bees
[184]	DJI Phantom 3	Mapir Survey 2 (Red and NIR bands)	Monitoring soil losses in olive orchards

PAN = panchromatic. MS = multispectral. DSMs = digital surface models. NIR = near-infrared. RGB = red-green-blue.

4. Identification and Mapping of Olive Groves

Land use is a coupled human-environment system that describes how the land is managed [75]. Land-cover mapping and monitoring represent one of the main applications of Earth-observing RS sensors data and are crucial for estimating land cover change [185]. Photo interpreters can use RS data for deriving land use information by using patterns, textures, or shapes [186]. Researchers recognized the importance of mapping land use and creating databases for sustainable natural resource management on local, regional, and national scales [187,188]. In addition, knowledge of soil's physical, biological, and chemical properties allows for the design and implementation of essential operations in PA, such as irrigation, drainage, nutrient, and other crop management strategies [89]. Furthermore, the importance of determining land uses is related, for example, to European financial support to agricultural producers via several subsidies [189], the implementation of specific agro-environmental measures, and the assessment of the impacts of existing management and policies at regional and national scales. An example of the first research in the early 2000s concerning this topic on olive groves was given by De Bruin [82], which presented an approach for predicting the areal extent of land cover types. In particular, the author proposed a geostatistical method to model spatial uncertainty in estimating the area extent of land cover types (including olive groves) derived from Landsat Thematic Mapper data.

Based on the European Union and national regulations for the subsidy of the creation of cover crops between rows of olive groves, Peña-Barragán et al. [64] evaluated RS techniques for a rapid and accurate assessment of cover crops in olive groves at a farm and regional level. The objectives of this research included determining the suitable time of the year for taking aerial photographs and the better VIs for discriminating different land uses. Results showed that the cover crop could not be distinguished from olive trees in spring, while both can be distinguished from bare soil. Regarding the detection of olive trees, among the VIs obtained by combining the Blue, Red, Green, and NIR bands, the best proved to be the following ratio: R/(B+G), able to detect olive trees in summer with an accuracy of almost 93%. Similar results in terms of accuracy were obtained in [65], developing a land cover classification using satellite imagery. In this case, based on the use of Quickbird images, the following objectives were pursued: selecting VIs for distinguishing each land cover; defining image processing sequences to automatically complete the separation and quantification of each land cover, among which olive groves. Land cover was randomly determined and georeferenced, carrying out field inspections to validate the classification procedure by tracing training zones to define the digital boundary values used in the classification routines. Classified regions were created with each land cover or grouping of land covers with similar digital value characteristics. The following bands, band ratios, and VIs were tested to discriminate land covers: Blue, Green, Red, NIR, Ratio Vegetation Index (RVI) [190], Blue/Green, Blue/Red, Red/Green, NIR/Blue, NIR/Green, Normalized Difference Vegetation Index (NDVI) [56], Adapted Soil Adjusted Vegetation Index (ASAVI) and Adapted Burnt Area Index (ABAI). A supervised classification method was employed to distinguish land covers by creating classified regions defined using the digital boundary values. In the case of olive groves cover class, it was identified by deleting the area resulting from the merging of the three classes' vegetation (consisting of the spring-sown herbaceous crops and vineyards plus roadside trees classes), non-vegetation (consisting of the bare agricultural soil and urban soil plus highways classes) and non-burnt stubble. Olive groves' cover crops were estimated by exploiting the NDVI to discriminate the olive trees and the Blue/Red ratio to discriminate cover crops, as shown in [64].

Weissteiner et al. [191] showed another methodology for classifying olive groves according to management intensity using agro-economic (such as yields) and ecological parameters (e.g., ground coverage and tree density). The input data were derived from a long-term time series of NOAA AVHRR (Advanced Very-High-Resolution Radiometer of National Oceanic and Atmospheric Administration) and calculation of the index Green Vegetation Fraction (GVF, [192]). Vegetation variables were derived from the parametrization of a long-term RS time series of GVF using a model called SINFIT. This model obtains parameters for quantifying

the component of permanent vegetation and that which changes seasonally. These parameters allow classifying the olive grove according to the intensity of management.

Torkashvand and Shadparvar [193] focus on identifying and mapping olive in Iran's Roodbar region using Indian Remote Sensing (IRS) images and GIS. Two methods were used: providing spectral reflectance stochastic (DN) of different land covers and supervised classification for discriminating olive groves from other land covers. For the first method, a training map was prepared and superimposed on a color composite sample consisting of three bands. In supervised classification, four methods were used: Box Classifier, Maximum Likelihood, Minimum Distance, and Minimum Mahalanobis distance. Dense olive groves were differentiated from low-dense groves. The results showed less accuracy and precision in classifying low-density olive groves due to the interference of the spectral signature of the canopies with those of other vegetation and soil cover.

The monitoring of land use over time and, in particular, the abandonment of olive growing or the reduction of land has been addressed by Efe et al. [83], which investigated land-use change on olive tree cultivation in the Edremit region in the northwest of Turkey. This research focused on the relationship between the natural environment and humans over three decades (1979–2006). Both historical maps and satellite imagery provided the data. In detail, topographic maps at 1:25,000 scale were used for land use determination in 1979, while Landsat Enhanced Thematic Mapper Plus (ETM+) images were used for land use determination in 2006. Field surveys were carried out to confirm land use. Changes in olive areas were determined by overlaying the surveyed data from 1979 and 2006. These data were overlayed with DEM to show changes in the olive groves according to the elevation levels. The tabular data expressed in hectares showed that in cases where areas occupied by olive groves were allocated to other agricultural uses, almost 74% of these areas were located at an altitude between 0 and 100 m. Moreover, the highest percentage (nearly 98%) in converting olive groves into residential areas is on the coast (0–100 m). This resulted in the centralization of olive groves located in marginal lands with severe productive use limitations, soil limitations, high altitude variation, and unfavorable ecological conditions.

Ghaderpour et al. [61] monitored vegetation variation (olive groves) through the least-squares wavelet analysis (LSWA), a time series analysis method developed by [194]. Four regions of Tunisia with different characteristics have been chosen: the first region was selected to study the relationship between the olive tree growth rate and temperature and precipitation; the second region was selected because it was occupied by a forest area that faces substantial degradation due to anthropogenic activities; the third region was selected because it was affected by the growth of salt-loving plants and a large number of migrant birds; the fourth region was chosen due to the vegetation cover degradation caused by the urban sprawl. The Landsat 7 Enhanced Thematic Mapper Plus (ETM+) satellite images, acquired for the period from 2000 to 2018, were used to create the NDVI time series. The results showed that NDVI time series of olive tree vegetation are highly coherent with temperature and precipitation time series.

Table 4 shows the researches in RS in olive growing dealing with the identification and mapping of olive groves.

Table 4. References dealing with the identification and mapping of olive groves.

Reference	Platform	Sensor Type Used	Aim of the Study
[82]	Satellite Landsat 5	MS	Predicting the areal extent of land-cover types
[83]	Satellite Landsat 7	MS	Monitoring land use changes
[61]	Satellite Landsat 7	MS	Change detection
[64]	Aircraft CESSNA 310 R	WILD RC-10 (RGB)	Assessing land-use in olive groves
[65]	Satellite Quickbird	MS	Discriminating land uses
[193]	Satellite Indian Remote Sensing	MS	Mapping olive groves
[191]	Satellite NOAA AVHRR	MS	Classifying olive groves according to management intensity

MS = multispectral. RGB = red-green-blue.

5. Olive Oil Mill Wastes (OOMW) Management

The olive oil industry is crucial in Mediterranean countries, being a source of wealth and tradition and one of the fundamental sectors of agriculture in these countries [34]. However, the extraction of olive oil produces a considerable quantity of waste harmful to the terrestrial and aquatic environment due to its phytotoxicity representing a critical environmental issue, especially in Mediterranean areas [195]. The extraction of olive oil consists of washing the olives, grinding, beating, and the extraction itself, representing the fundamental phase of the entire process [196]. Waste from oil mills can be divided into solid, olive husks, and a liquid component, OOMW [40]. The specific physicochemical characteristics of OOMW are variable, depending on climatic conditions, the cultivars from which the oil comes, the degree of ripeness of the olives, storage times, and the type of extraction [197–199]. The effects of OOMW on physicochemical soil properties also depend on the quantity, the time, the spreading method, and the surface slope [200]. OOMW could be temporarily stored in evaporation ponds or lagoons and then distributed evenly over agricultural land [201–204]. In European countries, the direct discharge of OOMW into rivers, lakes, sewer systems, and soils is strictly prohibited because of its harmful effects on the ecological balance [205]. However, this ban is often not respected. The impact of OOMW on aquatic ecosystems caused by phenols release, eutrophication, dissolved oxygen reduction, and pH alterations are well known [206,207]. On the other hand, infiltration of vegetation water into the soil affects carbonate distribution and can change pH, electrical conductivity, and nutrient content [40]. In soils covered by crops, OOMW causes many microorganisms' inhibition, reduced seed germination, and altered soil characteristics such as porosity and humus concentration [208]. To minimize environmental impact, OOMW must be processed. In this regard, research is oriented toward developing treatment technologies through physical, chemical, and biological processes [209]. Regarding the solution involving distribution on agricultural land, research found that OOMW application performs a positive effect on soil properties, if applied at controlled rates [210–214]. For example, as highlighted by Koutsos et al. [215], the adoption of sustainable practices can convert OOMW from a pollutant to a valuable resource, useful as an amendment in the context of sustainable agriculture. In this framework and concerning the problem described above, the RS can help detect OOMW disposal areas. The identification of the ground investigation is long and expensive [34]. In this regard, several researches have included the use of satellites providing medium and high-resolution imagery to achieve this objective [34, 38,40,47,57]. Alexakis et al. [40,47] developed an integrated geoinformatics approach for monitoring the land pollution in Crete (Greece) caused by the OOMW disposal. The proposed approach includes three steps: satellite RS data acquisition and processing (Landsat 8 OLI and IKONOS), geophysical prospection, soil/water sampling/chemical analysis. Firstly, mapping was carried out, detecting about 1300 OOMW tanks (topographically mapped). Hundreds of OOMW disposal areas were detected by using high-resolution satellite images of Google Earth, and more than 1000 sites were visited to record their position. Some different VIs were tested to evaluate their ability to identify disposal areas. The authors also proposed a detection index (DI) to improve the disposal areas' spectral response in Landsat's images. Results showed that Enhanced Vegetation Index (EVI) [44] and Difference Vegetation Index (DVI) [39] performed best. However, the spectral variance of OOMW makes their classification and detection difficult because of the mixed pixel phenomenon. Agapiou et al. [38] analyzed the spectral variance of the different components of olive oil wastes to identify the most suitable spectral windows for their detection. In particular, they tested GeoEye 1 imagery coupled with spectroradiometric ground measurements (between 350 and 1050 nm). Separability analysis showed that Blue and NIR bands represent the two optimal wavelengths "regions" for OOMW detection. The Blue Normalized difference vegetation index (BNDVI) [37], including in its formula Blue and NIR bands, was proposed for detecting OOMW disposal areas.

Agapiou et al. [57] investigated the potential suitability of very high-resolution satellite images (Pléiades, SPOT 6, Quickbird, WorldView-2, GeoEye 1) with a spatial resolution between 0.4 m and 1.5 m for detecting OOMW disposal areas by testing two indices:

NDVI and BNDVI. The tests showed that OOMW disposal areas, characterized by low values of both indices, can be recognized in most satellite images as black targets. In addition to optical satellite images, the COSMO-SkyMed radar image was preliminarily tested and fused with the hyperspectral Earth Observing-1 Advanced Land Imagery with a medium resolution image (30 m), proving its potential suitability for the detection of OOMW disposal areas, although it needs further studies.

Issaoui et al. [41] tested imagery of satellites Sentinel-2 and PlanetScope for monitoring OOMW disposal sites in two sites in Tunisia and Greece. Some VIs, NDVI, Normalized Difference Water Index (NDWI) [216], and DI were tested to evaluate their efficiency in detecting OOMW disposal areas. Image processing methods, false-color composites (FCC), Principal Component Analysis (PCA), and image fusion were applied to satellite images with the aim of improving the monitoring of OOMW ponds. The classification algorithms ISODATA, the Maximum Likelihood, and the Support Vector Machine (SVM) were used to assist in the overall approach of detection. Results showed that the optimum bands for monitoring OOMW are the NIR bands. PlanetScope imagery proved to be ideal for monitoring disposal sites, and Sentinel's medium-resolution (but free) images demonstrated to be used in some cases with successful results for this purpose.

Karydas et al. [217] developed a methodology that allows for a dynamic cause–effect linking of pollution sources and affected areas through OOMW pathways. Dataset used included a Quickbird image, a DEM, and olive oil production data. The first step of the methodology involves the creation of a database including possible sources of pollution (oil mills and tanks, mapped with photo-interpretation of false-color band composition Quickbird's image), and hydrogeological characteristics of the territory; determination of a set of risk parameters on the source scale by assigning to each source a risk value calculated by Multi-Criteria Analysis and Simple Additive Weighting method; allocation of all potentially impacted sites in the streams (receptor scale), calculating the risk values at the allocated sites by summing up the risk values of the sources for each of the impacted sites; calculation of the risk values for each watershed, summarizing risk values of the impacted sites included in the specific watershed. The result produced an assessment of the environmental risk caused by mill wastes at three different scales starting from the possible sources of pollution (mill units or wastewater tanks) to the mapping of impacted stream sites and finally considering the watershed as a whole.

Given the potential damage that OOMW can cause to aquatic ecosystems, Elhag et al. [218] mapped and evaluated the environmental pollution risks caused by OOMW discharged into surface stream networks. Firstly, the authors detected source points of pollution by visual photointerpretation using Quickbird's images. Land cover data and DEM were used to produce a hydrological model in which the prior location of the steepest downhill neighbor for each pixel of the DEM allows for the definition of the direction of movement of a water droplet from each pixel of the DEM. In this way, it was possible to simulate the surface movement of the OOMW according to the area's topography. The stream power index (SPI) was used to detect flat drainage areas susceptible to sedimentation.

Table 5 shows the researches in RS in olive growing dealing with the OOMW management.

Table 5. References dealing with the olive oil mill wastes (OOMW) management.

Reference	Platform	Sensor Type Used	Aim of the Study
[38]	Satellite GeoEye 1	MS	Spectral analysis of the different components of OOMW
[57]	Satellites Pleiades, SPOT 6, Quickbird, WorldView-2, GeoEye 1, COSMO-SkyMed	MS	Detection of OOMW disposal areas
[40,47]	Satellites Landsat 8 and IKONOS	PAN-MS	Detection of OOMW disposal areas
[218]	Satellite Quickbird	PAN-MS	Evaluation of the environmental pollution risks
[41]	Satellites Sentinel-2 and PlanetScope	MS	Detection of OOMW disposal areas
[217]	Satellite Quickbird	PAN-MS	Assessing and mapping risk of OOMW discharge to streams

PAN = panchromatic. MS = multispectral. OOMW = olive oil mill wastes.

6. Irrigation Water Management

Although olive trees are drought-tolerant species with specific anatomical adaptations and physiological mechanisms which allow for maintaining their vital functions under extreme stress [219], their distribution in arid regions is limited by annual rainfall of less than 350 mm, and water availability is an essential resource for improving final yields [158,220]. Therefore, rainfall's fundamental role in the economic profitability of this crop is evident, which can be exacerbated by arid summers [221]. In the typical Mediterranean areas of cultivation, where the climate is characterized by low and highly variable precipitation during the growing season and high potential evaporation, the lack of water is the main limiting factor for both the growth and productivity of the crop [8,222,223]. The characteristics of the soil also play an essential role in retaining water and thus in the growth of the olive tree [223]. Although it has adapted to poor, shallow soils, the olive tree prefers fertile, deep soils with moderate water content [12]. Indeed the olive groves mainly present on marginal soils with low water retention capacity and poor nutrient levels are characterized by compromised development and low yields [224]. Water stress can cause negative consequences, including low leaf area, limited photosynthesis, low flowering and fruiting, flower abortion, and cluster abscission [158,225].

Irrigation exploited to achieve greater production and economic competitiveness started to spread in the early 2000s and be used in traditional and modern olive groves showing positive effects on yield, fruit size, pulp-to-stone ratio, and oil content [220,222,226–230]. The high plant density, the scarcity of water resources for irrigation, and the high rainfall variability from year to year make localized irrigation and water deficit irrigation strategies necessary to maintain acceptable production levels [13,231]. Among the advantages of localized irrigation are the reduction of irrigation volumes because the entire soil surface is not irrigated. Consequently, the water savings can be used to increase the irrigated area or allocated to other uses [165]. However, to save water resources in agriculture, it is essential to improve water productivity, which corresponds to the ratio of yield (marketable product or net income) to the water used by the crop [232–234]. In woody crops such as olives, for which the production objective is not biomass, the most significant water productivity can be achieved with water deficit irrigation rather than full irrigation [235]. Deficit irrigation strategies are becoming widely used in modern olive groves to improve yield while maintaining low water consumption [236]. Optimizing water deficit irrigation involves obtaining the best balance between yield, olive oil quality, and irrigation water savings [236,237]. Among the advantages of the irrigation deficit, one is the improvement of the quality and derivatives of the fruits (such as olive oil) and the control of growth that allows reducing the intensity of pruning as well as the need for phytosanitary treatments [223,235,238]. In this framework, precision irrigation is well suited to the olive tree, a holistic approach to managing irrigation in cases of reduced water availability and variability of soil characteristics [239,240].

Several methods based on plant variables have been developed to measure water status and schedule irrigation. Conventional strategies include measuring leaf or stem water status, stomatal conductance, or photosynthesis. Automatic methods provide continuous measurements based on sap flow, trunk diameter, and leaf turgor pressure [231]. Automated processes are preferred for precision irrigation to be implemented with data transmission systems for remote access [231]. Furthermore, these methods can be combined with remote imagery to manage differential irrigation in areas with different water requirements [239,241,242]. Although these methods allow for accurate water stress measurement, they have some limitations, among which is the inability to be applied over large areas. The knowledge about the response of the olive tree to water intake and stress and the use of sensors for monitoring the water status combined with RS images facilitates the introduction of precision irrigation in olive groves [71,235]. Table 6 shows researches in RS in olive growing dealing with irrigation and water management. As highlighted by several authors [112,243–245], thermal RS has an essential role in plant water stress detection. Aerial thermal RS imagery permits spatially continuous information on plant water status over a

wider area than that obtained from local measurements [246,247]. Thermal images enable the detection of water stress conditions of a plant. The closure of leaf stomata reduces transpiration and evaporative cooling, causing an increase in leaf temperature detectable by thermal sensors [140,243,248]. In this respect, the work of Sepulcre-Cantó et al. [66] investigated the high-spatial-resolution multi-channel airborne sensor's capability to detect water stress causing changes in olive groves' canopy temperature. Aerial imagery was collected by an airborne hyperspectral scanner (AHS) at 2.5 m spatial resolution, acquiring 80 spectral bands, including ten thermal bands used to derive LST. Temperature measurements on the ground were made using a hand-held thermometer. Water potential and stomatal conductance were measured using a Scholander pressure chamber and a steady-state leaf porometer, respectively, while ten infrared sensors were placed on ten trees to measure canopy temperature. The olive trees investigated were under three different irrigation treatments to obtain three different water stress conditions. Results showed a higher temperature in water-stressed trees than in well-watered trees suggesting the ability of the AHS thermal data to detect changes in canopy temperature as a function of water stress levels. The best results were obtained from measurements taken early in the morning due to the slight temperature differences between the soil and the vegetation and, consequently, less interference from the soil temperature. The results provided valuable insights into managing controlled irrigation methods using RS techniques. These results were confirmed by Sepulcre-Cantó et al. [30], who focused on determining the potential of thermal RS in detecting water stress and how it affects yield and fruit quality parameters in olive and peach orchards. Images taken by AHS allowed for the detection of differences in tree canopy temperature associated with irrigation levels. The yield and quality parameters oil content (over dry fruit weight), fruit water content, oil yield, and fresh fruit weight were considered. It was showed a high correlation between water stress and some parameters: fruit water content and fresh fruit weight. The link between detected temperature and water stress could allow to map potential yield indicators and some quality parameters. In addition, the medium resolution of the satellite sensor (ASTER) was simulated and tested for detecting water stress by reducing the spatial resolution of imagery taken by AHS. The test was performed through a simulation of the spectral characteristics of the ASTER sensor, aggregating the pixels of the canopy, soil and projected shadow. The high correlation between canopy and the air temperature difference (T_c-T_a), measured by AHS, and the temperature simulated for the spectral characteristics of the ASTER sensor demonstrated the potentialities of using medium-resolution satellite imagery for canopies'water stress monitoring.

ASTER's thermal imagery combined with VIs NDVI, greenness index (GI), Modified triangular vegetation index ($MTVI_1$) [50], $MTVI_2$ [50], Modified chlorophyll absorption in reflectance index ($MCARI_1$) [50], $MCARI_2$ [50], Modified Soil Adjusted Vegetation Index (MSAVI) [52], and Optimized Soil Adjusted Vegetation Index (OSAVI) [67] was used by Sepulcre-Cantó et al. [45] for the discrimination between irrigated and rainfed open-tree canopies olive groves. A radiative transfer simulation conducted with the DART model was used to simulate open orchards scene (among which olive trees), evaluating the effects of the vegetation cover, crown LAI, and background temperature on the canopy temperature exploited for discriminating between irrigated and rainfed olive groves. The authors positively assessed cases where irrigated groves had lower canopy temperatures (due to increased canopy conductance) and higher NDVI than non-irrigated groves. In particular, thermal differences of up to 2 K (Kelvin degrees) between irrigated and non-irrigated groves were evident in summer while they disappeared in winter satellite imagery.

In the Mediterranean, where the growing season is hot and dry, an accurate estimation of water needs is essential for better managing water resources in agriculture. For this reason, it is important to have a reliable estimate of daily evapotranspiration (ET) fluxes. Using airborne mounting MS and thermal cameras, Cammalleri et al. [58] tested an approach based on a modified version of the standard FAO-56 dual crop coefficient procedure to estimate ET in an area occupied by olive trees similarly to [249]. Estimating orchard water requirements allows for establishing irrigation management strategies to increase water

productivity and optimize the yield and quality of olive trees growing in water shortage conditions [250]. The calculation of ET is influenced by the intra-orchard spatial variability, such as canopy size, dependent on both the training system and soil water holding capacity [143]. The training system and canopy geometries may affect the partitioning of net radiation into sensible heat flux, soil heat flux, and latent heat flux. Ortega-Farías et al. [251] used MS and thermal UAV imagery to evaluate energy balance components' intra-orchard spatial variability. A field experiment was carried out to develop an RS energy balance (RSEB) algorithm for estimating olive evapotranspiration in a drip-irrigated grove. For implementing the RSEB algorithm, measurements of climatic variables (Ta, u, and Rha), UAV data, NDVI, and temperature were used. This research showed that UAVs alone, or if complemented with satellites, can estimate intra-field spatial variability of the energy balance components and water requirements.

Sobrino et al. [252] tested the reliability of thermal RS by analyzing the feasibility of retrieving LST (in a 4-ha irrigated olive orchard). The second objective was the evaluation of the accuracy obtained depending on the number of thermal bands used. The aerial surveys were carried out using a hyperspectral scanner with 80 bands distributed in four "regions" of the electromagnetic spectrum (visible, NIR, SWIR, Mid-wave infrared, and Long-wave infrared). The authors chose to test three methods for LST retrieval: the single-channel method, which exploits one thermal band; the two-channel method, which combines two thermal bands; temperature and emissivity separation (TES) method [253], which provides surface emissivity in addition to temperature by using MS and thermal data. Infrared sensors were placed on poles to monitor the temperature of the canopy as a function of a gradient in the water status of the olive trees obtained by the drip irrigation method. In particular, band 75 (10.07 μm) showed the highest atmospheric transmissivity using the single-channel method, which is the most suitable in this case. The combination of the bands 75 and 79 (12.35 μm) provided similar results by applying the two-channel method.

Some researches [63,84,88,254] stood apart from the others on water stress and concerns with the management of water resources in olive groves in arid areas (North African countries). Castelli et al.'s work [254] deals with the effect of jessour, traditional water harvesting check dams, on olive growing in Tunisia. Time series of Normalized Difference Infrared Index NDII [255] derived from Landsat 7 were retrieved from Google Earth Engine imagery for analyzing olive trees' water conditions over a period ranging from 1999 to 2017. Using a methodology that included ground-based soil moisture measurements, the authors confirmed the usefulness of NDII in representing the state of soil moisture in dry soil conditions, as shown by Sriwongsitanon et al. [256]. In addition, the monitoring showed that jessour sites reduce olive trees' water stress compared with non-jessour sites. Kefi et al. [84] detected irrigated and non-irrigated (rainfed) olive-growing farms in Tunisia using Landsat 8 imagery and analyzing temporal changes exploiting NDVI, RVI, and LST. The results showed the usefulness of NDVI and LST data in identifying irrigated olive-growing farms characterized in summer by higher vegetation index values and lower temperatures. Hoedjes et al. [88] aimed to calculate daily evapotranspiration using satellite imagery (ASTER) to improve irrigation water management at the field scale of an irrigated olive grove in Morocco. Kharrou et al. [63] evaluated an RS-based approach to estimate the temporal and spatial distribution of crop evapotranspiration (ET) and irrigation water requirements over irrigated areas in Morocco. The approach is based on the daily step FAO-56 Soil Water Balance model, which was combined with a time series (2002–2003 and 2008–2009) of basal crop coefficients and the fractional vegetation cover derived from Landsat TM satellite NDVI imagery. The model was calibrated and validated at a plot scale using ET measured by eddy-covariance systems in wheat fields and olive groves. The model showed to be able to provide reasonable estimates of ET both for wheat and olive.

Table 6. References dealing with irrigation water management.

Reference	Platform	Sensor Type Used	Aim of the Study
[139]	Aircraft CESSNA C172S EC-JYN	FLIR SC655 (TH)	Water stress detection
[140]	Aircraft -	Hyperspectral Scanner (HY)	Mapping canopy conductance and CWSI
	UAV	FLIR Thermovision A40 M (TH)	
[58]	Aircraft -	MS-TH	Measuring olive grove's evapotranspiration
[71]	Satellites Landsat 7–8	MS	Detecting differences in spectral response on the estimation of evapotranspiration
[254]	Satellite Landsat 7	MS	Monitoring effects of check dams on soil and olive tree water status
[60]	UAV -	MS	Delineating Management Zones
[88]	Satellite ASTER	TH	Calculating daily evapotranspiration
[48]	UAV DJI Phantom 4 Pro	Parrot Sequoia (MS)	Detection of irrigation inhomogeneities
[84]	Satellite Landsat 8	MS-TH	Detecting irrigated olive growing farms
[63]	Satellite Landsat 5	MS	Estimate the temporal and spatial distribution of crop evapotranspiration (ET) and irrigation water requirements
[257]	UAV -	EasIR9 (TH)	Water stress detection
[143]	UAV TAROT-1000 RC	FLIR Tau 2 640 (TH)	Estimating the intra-orchard spatial variability
[258]	UAV senseFly eBee	senseFly Thermomap (TH)	Estimation of olive canopy and soil surface temperatures, under different irrigation treatments
[232]	UAV—DJI Mavic Pro 2	Hasselblad L1D-20c (RGB)	Detecting different irrigation systems
	UAV DJI Matrice 600 Pro	Nano Hyperspec (HY)	
[66]	Aircraft -	Hyperspectral scanner (TH-HY)	Water stress detection
[30]	Aircraft - Satellite ASTER	Hyperspectral scanner (TH-HY)	Monitoring yield and fruit quality parameters in groves under water stress
[45]	Aircraft - Satellite ASTER	Hyperspectral scanner (TH-HY)	Discrimination of irrigated and rainfed tree orchards
[252]	Aircraft CASA 212–200	Hyperspectral scanner (TH-HY)	Measuring land surface temperature

MS = multispectral; TH = thermal; HY = hyperspectral; - = missing information. CWSI = Crop Water Stress Index. RGB = red-green-blue.

The lack of high spatial and temporal resolution of satellite thermal images makes them unsuitable for the estimation of water requirements of the olive tree in some phenological phases [143]. In the last decade, the first studies based on UAVs mounting thermal (and MS or hyperspectral) cameras for applications in agriculture can be found. Crop irrigation management became a crucial application of UAV technologies in PA [119]. UAVs, equipped with several sensors, among which are thermal, can detect possible deficiencies in the irrigation of different sites. These data can be processed through photogrammetry techniques to produce a high-resolution vegetation map highlighting the water-stressed areas. The detection of water stress was studied in different tree species, including the olive tree, together with the estimation of orchards' water requirements [48,140,141,143,232,257,258]. To our knowledge, a couple of researches on olive trees [139,140] have used UAV thermal images exploiting the Crop Water Stress Index (CWSI). CWSI [246] is a temperature-based index that can assume values between 0 and 1 and is directly proportional to the water stress level of many species of interest in agriculture. In several studies, CWSI was shown to have good correlations with leaf water potential (Ψ_L) [229,259,260]. Berni et al. [140] used thermal imagery (taken by UAV and airborne) to calculate and map the tree canopy

conductance and the CWSI in a heterogeneous olive orchard by combining the energy balance equations and the theoretical formulation of CWSI.

Bellvert et al. [139] compared CWSI derived from thermal UAV imagery and leaf water potential (Ψ_L) measured using a Scholander pressure chamber in olive trees. The linear relationships between CWSI and Ψ_L allowed for the remote estimation of Ψ_L and the detection of spatial variability of plant water status in an olive orchard. Similarly, Egea et al. [141] proved the usefulness of the CWSI, both obtained by thermal UAV imagery and field measurements, for monitoring water stress in a super-intensive olive grove by evaluating relationships between CWSI and other water stress indicators, such as stomatal conductance, stem water potential, and leaf transpiration rate.

Scholander pressure chamber can provide accurate knowledge of olive water status [261] but is impractical due to the large number of measurements required [262]. The same applies to the calculation of stomatal conductance [263]. Taking into account the need, in the framework of PA, to overcome these limitations, Poblete-Echeverría et al. [257] evaluated the accuracy of water stress detection performed using aerial and terrestrial infrared thermography in a vineyard and in an olive grove. Field measurements included calculating Ψ_{stem} on several twigs while canopy temperature was measured using a hand-held thermal camera (lateral imagery) and UAV for nadir-view thermal imagery. Results showed that the difference between the canopy's temperature and air temperature (T_c–T_a) was related to differences in water potential for different irrigation treatments when the olive was under stress.

Riveros-Burgos et al. [143] used UAV thermal imagery and meteorological data to estimate the intra-orchard spatial variability in olive water requirements in super-intensive drip-irrigated orchards. For this purpose, the authors used the clumped model of Brenner and Incoll [264], which is considered suitable for producing maps to estimate the intra-orchard spatial variability in the presence of heterogeneous canopies (typical of intensive and super-intensive groves), which influences the partitioning of ET into tree transpiration and soil surface evaporation.

Using sensors other than thermal ones allows the discrimination of management zones, irrigation inhomogeneities, and irrigation methods based on the olive tree's spectral response, as shown in [48,60,232]. Gertsis et al. [60] used NDVI, obtained from RS ground-level measurements, and UAV to identify different areas in crops grown and to delineate Management Zones in an olive orchard in Greece. Jorge et al. [48] compared several VIs (NDVI, NDRE, Green Normalized Vegetation Index GNDVI [46], and Soil Adjusted Vegetation Index SAVI [70]) using MS UAV imagery for detecting inhomogeneities in irrigated vineyards and olive groves. According to their results, the NDRE (Normalized Difference Red Edge Index) [265] highlighted irrigation irregularities more effectively. Santos-Rufo et al. [232] used UAV hyperspectral data to compare the performance of some wavelength selection methods based on Partial Least Square (PLS) regression [266,267] to discriminate two systems of irrigation used in olive groves: subsurface drip irrigation and surface drip irrigation. As the spectral response of the olive trees is sensitive to the irrigation technique used, the authors were able to map the irrigated areas.

7. Final Remarks and Conclusions

This review covered the past, from the 2000s onwards, and the most recent applications of aerial RS technology in olive growing. To the best of our knowledge, we are the first to focus on this specific topic. Starting synthesis on RS platforms and sensors, mainly satellites and UAVs used in research, is followed by the discussion of several topics by reviewing research conducted over the twenty years analyzed, from the protection of the olive-growing landscape from erosion and pollution.

Concerning the platforms used, overall, the use of satellite data is equivalent to that of UAV images, with a prevalence of one of them according to the specific topic and objectives in olive growing. Considering the several factors to consider when comparing platforms and sensors, both technical (spatial, temporal, and radiometric resolutions, areal coverage,

targeted features) and economic (UAV equipment vs. satellite images costs), it is complex to evaluate and suggest what would be the best approach to use in a survey [268]. Indeed, in the early 2000s, most of the research involved satellite and aircraft imagery, used for mapping and inventorying olive groves, as it was still early for the spread of UAVs and their use in agriculture [269].

In light of the researches reviewed, the identification of olive groves and OOMW management monitoring concerned the predominant use of satellite imagery over aircraft and UAVs. One of the main advantages of satellite imagery is the possibility of covering large areas. In particular, providing data over large areas with spatial resolutions ranging from 30 m of Landsat to less than 4 m using IKONOS and Quickbird allowed for achieving remarkable results in the topics addressed by the research in the first decade of 2000. Moreover, Landsat imagery remains a reliable data source for studying land-use changes because of its relatively high spatial resolution and long-term archives, now reaching fifty years (considering the first images since 1972). However, even though significant progress has been made in developing high-resolution satellite sensors since 1999, some challenges remain. Many satellites capable of providing high-resolution images close to or below one meter belong to commercial companies, which means costs for a farm to obtain and reuse images. To date, the highest spatial resolution images free of charge are those provided by the Sentinel satellites. In addition, although many satellites provide images of an area with a temporal resolution of between one and five days, it is necessary to consider the local weather conditions that may prevent obtaining long periods of continuous images of acceptable quality [270]. Therefore, integrating images from various satellites to create high-quality, dense time-series data becomes a critical task for studies requiring observations with high frequency and high spatial resolution [271]. Because multiple satellite sensors are available, potential customers can order images provided by more than one satellite sensor, increasing the possibility of having images rapidly despite the difficulties posed by the cloudiness and the different revisit frequencies of a specific area. The introduction of new, relatively recent platforms, including nano-satellites, and mounting sensors providing high or ultra-high resolution images, less than 3 m and 1 m, respectively, have made satellites more competitive with UAVs in PA applications [15]. However, to our knowledge, only three papers dealing with olive groves used nanosatellite images such as Cubesats from PlanetScope [41,98,99]. This is despite the affordable price of the images compared to satellites with similar or higher resolution, such as Pleiades and WorldView [272]. In the topics of olive grove identification and management of OOMW, the preponderant role of satellites in achieving the objectives and in reducing the complexity of environmental monitoring can be observed even in those without both high spatial and temporal resolution. Imagery from satellites capable of "covering wide areas" can be used primarily at the territorial level, and in olive growing, for monitoring large olive groves with "traditional" planting distances such that individual canopies can be distinguished by public administrations and control bodies [33]. To better exploit the wide variety of publicly available satellite data and produce high temporal and spatial resolution data, several data fusion approaches have been proposed that can combine high/medium spatial resolution data with high temporal resolution data [271]. Satellites have difficulty producing images that have both high spatial and temporal resolution because of the tradeoff between scan width and pixel size [273]. In this regard, a novelty is constituted by a constellation of satellites soon to be launched called WorldView Legion, which will consist of six satellites capable of providing images at a resolution of less than 30 cm and with high frequency (up to 15 times per day) on the areas most in demand (www.maxar.com, last access 3 October 2022). Images from aircraft, which present better quality than satellite images, can also be used in PA [114]. Like the other platforms, the limitations dictated by weather conditions and, concerning the areas covered, by the presence or absence of companies that provide RS imagery services remain, in addition to the costs not accessible to all users [89,119]. It is desirable that the use of RS platforms and sensors in agriculture is not only the prerogative of research institutions but that it continues the trend of increasing user-friendliness of these technologies for all types

of users. Motivating and developing the skills of a wide variety of farmers may be the main challenge toward real-world applications of RS platforms in agriculture. However, proper use of the technologies requires increasing farmer confidence and knowledge even when using a more readily available platform such as the UAV. Training to implement the entire workflow, including the proper use of sensors, is critical in the instrumentation's use and repair and maintenance aspects [148]. Cheaper, consumer-grade optical (RGB) sensors are not always suitable for agricultural applications. NIR-equipped MS sensors are needed for calculating many VIs, just as thermal cameras are critical in water stress monitoring. Furthermore, using more complex sensors, such as LiDAR and hyperspectral cameras, often requires a higher load capacity from the UAV and a consequent higher expense in purchasing the RS platform. Beyond a desirable and probable lowering of the weight and cost of UAVs and sensors in the future, the considerations made so far are essential to understanding the current user base that can afford this technology. Outside the scope of research, the farms with greater economic resources and extensions are certainly more facilitated and interested in the purchase of UAV and its use for crop monitoring (including equipment cost and data processing through a specific software). In addition, the training required to implement the entire workflow in the data acquisition and processing phases is of paramount importance. Critical steps that can be improved, mainly on automation, include preparing the optimal flight plan, configuring and calibrating sensors before and during flight, in the case of UAV data, and reducing the time required for data processing. From this, it follows that using RS technologies in agriculture demands both in phases of acquisition and processing the presence of expert and qualified experts with aggravation of expense for the company. Unlike satellites whose applications are generally associated with a processing chain that ensures final data quality, images from UAVs require several sometimes complex steps to be retrieved and used after surveying [274].

For this reason, adopting UAV technologies by individual farmers with few and small agricultural fields is less common [119]. It is desirable that continued development of sensor technologies, lower costs, and input cost savings will bring benefits that will make it easier to overcome this obstacle in the future. So far, if compared to satellites, UAVs have been shown to provide significantly better spatial resolution imagery and greater flexibility in selecting the appropriate spatio-temporal resolution [275]. Compared to aircraft, UAVs can fly at lower altitudes and, in the case of monitoring performed on tree species, fly closer to tree tops and provide a very detailed view of the dynamics of the vegetation [276]. The application of UAVs in aerial photogrammetry is accepted as a reliable and accurate remote sensing method for environmental protection and mapping vegetation species, including the olive tree.

The preservation of olive groves as an element of Mediterranean identity both in landscaping and as a strategic economic resource in agriculture depends on sustainable environmental management based on improving the competitiveness of the agricultural sector and technological progress in compliance with the guidelines of PA [97,277,278]. Landscapes should be regarded as a land-use system at the center of human-nature relations that to be managed efficiently to preserve and restore ecosystem services while contributing to sustainable solutions, including the challenge of food security [279,280]. Characterization of agricultural systems with a focus on agricultural intensification is useful for understanding the sustainability of agricultural lands. In this framework, the contribution of RS is important, as shown in the applications seen in landscape monitoring and soil defense, olive grove monitoring, and OOMW management. Coupled with the challenges facing olive growing and agriculture, more generally in terms of production, are those related to climate change, the most obvious consequences of which include a changing distribution of rainfall and an increasing number of extreme weather events, and increased environmental pressures represented by the risks of overexploitation of groundwater resources, degradation of water and soil quality [77,223]. Among the uses of RS, beyond the type of platform employed, the synthesis between the need to meet the needs of consumers and producers in terms of economic as well, while at the same time

preserving the environment and its resources is represented by its use in water resource management. RS has been shown both to be able to contribute to the defense of water bodies from wastewater pollution risk (citation) and, through the determination of irrigation inhomogeneities, spatial variability within the orchard, evapotranspiration, etc., to be able to give guidance for irrigation optimization in the balance between yield, product quality, and equitable consumption of water. In pursuit of these goals, an already well-established use of RS in olive crop research becomes evident and equally desirable on farms, in line with the key principles of PA, i.e., " . . . support management decisions according to estimated variability for improved resource use efficiency, productivity, quality, profitability and sustainability of agricultural production" and the present and future needs of the olive sector [281].

Author Contributions: Conceptualization, methodology, investigation, data curation, writing—review and editing, G.M. (Gaetano Messina) and G.M. (Giuseppe Modica). All authors have read and agreed to the published version of the manuscript.

Funding: This research received no external funding.

Conflicts of Interest: The authors declare no conflict of interest.

References

1. Kaniewski, D.; Van Campo, E.; Boiy, T.; Terral, J.F.; Khadari, B.; Besnard, G. Primary domestication and early uses of the emblematic olive tree: Palaeobotanical, historical and molecular evidence from the Middle East. *Biol. Rev.* **2012**, *87*, 885–899. [CrossRef] [PubMed]
2. Zohary, D.; Hopf, M.; Weiss, E. *Domestication of Plants in the Old World: The Origin and Spread of Domesticated Plants in Southwest Asia, Europe, and the Mediterranean Basin*; Oxford University Press: Oxford, UK, 2012; ISBN 9780191810046.
3. Loumou, A.; Giourga, C. Olive groves: "The life and identity of the Mediterranean". *Agric. Hum. Values* **2003**, *20*, 87–95. [CrossRef]
4. Carrión, Y.; Ntinou, M.; Badal, E. *Olea europaea* L. in the North Mediterranean Basin during the Pleniglacial and the Early-Middle Holocene. *Quat. Sci. Rev.* **2010**, *29*, 952–968. [CrossRef]
5. Blondel, J.; Aronson, J.; Bodiou, J.-Y.; Boeuf, G. *The Mediterraneaen Region—Biological Diversity in Space and Time*; Oxford University Press: Oxford, UK, 2010; p. 401.
6. Besnard, G.; Khadari, B.; Navascués, M.; Fernández-Mazuecos, M.; El Bakkali, A.; Arrigo, N.; Baali-Cherif, D.; Brunini-Bronzini de Caraffa, V.; Santoni, S.; Vargas, P.; et al. The complex history of the olive tree: From late quaternary diversification of mediterranean lineages to primary domestication in the northern Levant. *Proc. R. Soc. B Biol. Sci.* **2013**, *280*, 20122833. [CrossRef] [PubMed]
7. Zohary, D.; Spiegel-Roy, P. Beginnings of fruit growing in the Old World. *Science* **1975**, *187*, 319–327. [CrossRef]
8. Fiorino, P. *Olea. Trattato di Olivicoltura*; Edagricole—Edizioni Agricole di New Business Media srl: Bologna, Italy, 2018; ISBN 978-88-506-4938-9.
9. Urieta, D.; Menor, A.; Caño, S.; Barreal, J.; Del Mar Velasco, M.; Puentes, R. *International Olive Growing Worldwide Analysis and Summary*, 1st ed.; Fundación Caja Rural de Jaén: La Carolina, Spain, 2018; Available online: https://www.researchgate.net/publication/326070870_INTERNATIONAL_OLIVE_GROWING (accessed on 2 October 2022).
10. Lanza, B.; Poiana, M. Olive da Tavola: Tecnologia. Available online: https://www.accademiaolivoeolio.com/img2/file/lanza-b-e-poiana-m-olive-da-tavola_201804051130159_5u30nvg1r5mn90ttqbmus2tw4.pdf (accessed on 15 March 2022).
11. FAO. FAOSTAT. Available online: https://www.fao.org (accessed on 1 February 2022).
12. Therios, I. *Olives: Crop Production Science in Horticulture 18*; CABI International: Wallingford, UK, 2009.
13. Rallo, L.; Caruso, T.; Diez, C.; Campisi, G. Olive Growing in a Time of Change: From Empiricism to Genomics. In *The Olive Tree Genome*; Springer: Cham, Switzerland, 2016; pp. 55–64. ISBN 978-3-319-48887-5.
14. Colomina, I.; Molina, P. Unmanned aerial systems for photogrammetry and remote sensing: A review. *ISPRS J. Photogramm. Remote Sens.* **2014**, *92*, 79–97. [CrossRef]
15. Messina, G.; Peña, J.M.; Vizzari, M.; Modica, G. A Comparison of UAV and Satellites Multispectral Imagery in Monitoring Onion Crop. An Application in the 'Cipolla Rossa di Tropea' (Italy). *Remote Sens.* **2020**, *12*, 3424. [CrossRef]
16. Maes, W.H.; Steppe, K. Perspectives for Remote Sensing with Unmanned Aerial Vehicles in Precision Agriculture. *Trends Plant Sci.* **2019**, *24*, 152–164. [CrossRef]
17. Duro, D.C.; Coops, N.C.; Wulder, M.A.; Han, T. Development of a large area biodiversity monitoring system driven by remote sensing. *Prog. Phys. Geogr. Earth Environ.* **2007**, *31*, 235–260. [CrossRef]
18. Turner, W.; Spector, S.; Gardiner, N.; Fladeland, M.; Sterling, E.; Steininger, M. Remote sensing for biodiversity science and conservation. *Trends Ecol. Evol.* **2003**, *18*, 306–314. [CrossRef]
19. Gillespie, T.W.; Foody, G.M.; Rocchini, D.; Giorgi, A.P.; Saatchi, S. Measuring and modelling biodiversity from space. *Prog. Phys. Geogr. Earth Environ.* **2008**, *32*, 203–221. [CrossRef]

20. Nagendra, H. Using remote sensing to assess biodiversity. *Int. J. Remote Sens.* **2001**, *22*, 2377–2400. [CrossRef]
21. Foody, G.M.; Atkinson, P.M.; Gething, P.W.; Ravenhill, N.A.; Kelly, C.K. Identification of specific tree species in ancient semi-natural woodland from digital aerial sensor imagery. *Ecol. Appl.* **2005**, *15*, 1233–1244. [CrossRef]
22. Haara, A.; Haarala, M. Tree Species Classification using Semi-automatic Delineation of Trees on Aerial Images. *Scand. J. For. Res.* **2002**, *17*, 556–565. [CrossRef]
23. Carleer, A.; Wolff, E. Exploitation of Very High Resolution Satellite Data for Tree Species Identification. *Photogramm. Eng. Remote Sens.* **2004**, *70*, 135–140. [CrossRef]
24. Salamí, E.; Gallardo, A.; Skorobogatov, G.; Barrado, C. On-the-fly olive tree counting using a UAS and cloud services. *Remote Sens.* **2019**, *11*, 316. [CrossRef]
25. Sarabia, R.; Aquino, A.; Ponce, J.M.; López, G.; Andújar, J.M. Automated identification of crop tree crowns from uav multispectral imagery by means of morphological image analysis. *Remote Sens.* **2020**, *12*, 748. [CrossRef]
26. Estornell, J.; Ruiz, L.A.; Velázquez-Martí, B.; López-Cortés, I.; Salazar, D.; Fernández-Sarría, A. Estimation of pruning biomass of olive trees using airborne discrete-return LiDAR data. *Biomass Bioenergy* **2015**, *81*, 315–321. [CrossRef]
27. Jiménez-Brenes, F.M.; López-Granados, F.; de Castro, A.I.; Torres-Sánchez, J.; Serrano, N.; Peña, J.M. Quantifying pruning impacts on olive tree architecture and annual canopy growth by using UAV-based 3D modelling. *Plant Methods* **2017**, *13*, 55. [CrossRef]
28. Díaz-Varela, R.A.; de la Rosa, R.; León, L.; Zarco-Tejada, P.J. High-resolution airborne UAV imagery to assess olive tree crown parameters using 3D photo reconstruction: Application in breeding trials. *Remote Sens.* **2015**, *7*, 4213–4232. [CrossRef]
29. Caruso, G.; Zarco-Tejada, P.J.; González-Dugo, V.; Moriondo, M.; Tozzini, L.; Palai, G.; Rallo, G.; Hornero, A.; Primicerio, J.; Gucci, R. High-resolution imagery acquired from an unmanned platform to estimate biophysical and geometrical parameters of olive trees under different irrigation regimes. *PLoS ONE* **2019**, *14*, e0210804. [CrossRef] [PubMed]
30. Sepulcre-Cantó, G.; Zarco-Tejada, P.J.; Jiménez-Muñoz, J.C.; Sobrino, J.A.; Soriano, M.A.; Fereres, E.; Vega, V.; Pastor, M. Monitoring yield and fruit quality parameters in open-canopy tree crops under water stress. Implications for ASTER. *Remote Sens. Environ.* **2007**, *107*, 455–470. [CrossRef]
31. Maselli, F.; Chiesi, M.; Brilli, L.; Moriondo, M. Simulation of olive fruit yield in Tuscany through the integration of remote sensing and ground data. *Ecol. Modell.* **2012**, *244*, 1–12. [CrossRef]
32. Sola-Guirado, R.R.; Castillo-Ruiz, F.J.; Jiménez-Jiménez, F.; Blanco-Roldan, G.L.; Castro-Garcia, S.; Gil-Ribes, J.A. Olive actual "on year" yield forecast tool based on the tree canopy geometry using UAS imagery. *Sensors* **2017**, *17*, 1743. [CrossRef] [PubMed]
33. Roma, E.; Catania, P. Precision Oliviculture: Research Topics, Challenges, and Opportunities—A Review. *Remote Sens.* **2022**, *14*, 1668. [CrossRef]
34. Agapiou, A.; Papadopoulos, N.; Sarris, A. Detection of olive oil mill waste (OOMW) disposal areas using high resolution GeoEye's OrbView-3 and Google Earth images. *Open Geosci.* **2016**, *8*, 700–710. [CrossRef]
35. Doula, M.K.; Moreno-Ortego, J.L.; Tinivella, F.; Inglezakis, V.J.; Sarris, A.; Komnitsas, K. *Olive Mill Waste: Recent Advances for the Sustainable Development of Olive Oil Industry*; Elsevier Inc.: Amsterdam, The Netherlands, 2017; ISBN 9780128053140.
36. Messina, G.; Modica, G. The role of remote sensing in olive growing farm management. A research outlook from 2000 to the present in the framework of precision agriculture applications. *Remote Sens.* **2022**, *in press*.
37. Wang, F.; Huang, J.; Tang, Y.; Wang, X. New Vegetation Index and Its Application in Estimating Leaf Area Index of Rice. *Rice Sci.* **2007**, *14*, 195–203. [CrossRef]
38. Agapiou, A.; Papadopoulos, N.; Sarris, A. Discriminant analysis of olive oil mill wastes using spectroradiometers in the visible and near infrared part of the spectrum. *Eur. J. Remote Sens.* **2015**, *48*, 793–809. [CrossRef]
39. Richardson, A.J.; Wiegand, C.L. Distinguishing vegetation from soil background information. *Photogramm. Eng. Remote Sens.* **1977**, *43*, 1541–1552.
40. Alexakis, D.D.; Sarris, A.; Kalaitzidis, C.; Papadopoulos, N.; Soupios, P. Integrated use of satellite remote sensing, GIS, and ground spectroscopy techniques for monitoring olive oil mill waste disposal areas on the island of Crete, Greece. *Int. J. Remote Sens.* **2016**, *37*, 669–693. [CrossRef]
41. Issaoui, W.; Alexakis, D.D.; Nasr, I.H.; Argyriou, A.V.; Alevizos, E.; Papadopoulos, N.; Inoubli, M.H. Monitoring Olive Oil Mill Wastewater Disposal Sites Using Sentinel-2 and PlanetScopeSatellite Images: Case Studies in Tunisia and Greece. *Agronomy* **2022**, *12*, 90. [CrossRef]
42. Lima-Cueto, F.J.; Blanco-Sepúlveda, R.; Gómez-Moreno, M.L.; Galacho-Jiménez, F.B. Using vegetation indices and a UAV imaging platform to quantify the density of vegetation ground cover in olive groves (*Olea europaea* L.) in Southern Spain. *Remote Sens.* **2019**, *11*, 2564. [CrossRef]
43. Beniaich, A.; Silva, M.L.N.; Guimarães, D.V.; Avalos, F.A.P.; Terra, F.S.; Menezes, M.D.; Avanzi, J.C.; Cândido, B.M. UAV-based vegetation monitoring for assessing the impact of soil loss in olive orchards in Brazil. *Geoderma Reg.* **2022**, *30*, e00543. [CrossRef]
44. Liu, H.Q.; Huete, A. A feedback based modification of the NDVI to minimize canopy background and atmospheric noise. *IEEE Trans. Geosci. Remote Sens.* **1995**, *33*, 457–465. [CrossRef]
45. Sepulcre-Cantó, G.; Zarco-Tejada, P.J.; Sobrino, J.A.; Berni, J.A.J.; Jiménez-Muñoz, J.C.; Gastellu-Etchegorry, J.P. Discriminating irrigated and rainfed olive orchards with thermal ASTER imagery and DART 3D simulation. *Agric. For. Meteorol.* **2009**, *149*, 962–975. [CrossRef]
46. Gitelson, A.A.; Kaufman, Y.J.; Merzlyak, M.N. Use of a green channel in remote sensing of global vegetation from EOS-MODIS. *Remote Sens. Environ.* **1996**, *58*, 289–298. [CrossRef]

47. Alexakis, D.D.; Sarris, A.; Papadopoulos, N.; Soupios, P.; Doula, M.; Cavvadias, V. Geodiametris: An integrated geoinformatic approach for monitoring land pollution from the disposal of olive oil mill wastes. In Proceedings of the Second International Conference on Remote Sensing and Geoinformation of Environment, Paphos, Cyprus, 7–10 April 2014; Volume 9229. [CrossRef]
48. Jorge, J.; Vallbé, M.; Soler, J.A. Detection of irrigation inhomogeneities in an olive grove using the NDRE vegetation index obtained from UAV images vegetation index obtained from UAV images. *Eur. J. Remote Sens.* **2019**, *52*, 169–177. [CrossRef]
49. Gitelson, A.A.; Kaufman, Y.J.; Stark, R.; Rundquist, D. Novel algorithms for remote estimation of vegetation fraction. *Remote Sens. Environ.* **2002**, *80*, 76–87. [CrossRef]
50. Haboudane, D.; Miller, J.R.; Pattey, E.; Zarco-Tejada, P.J.; Strachan, I.B. Hyperspectral vegetation indices and novel algorithms for predicting green LAI of crop canopies: Modeling and validation in the context of precision agriculture. *Remote Sens. Environ.* **2004**, *90*, 337–352. [CrossRef]
51. Chen, J.M. Evaluation of vegetation indices and a modified simple ratio for boreal applications. *Can. J. Remote Sens.* **1996**, *22*, 229–242. [CrossRef]
52. Qi, J.; Chehbouni, A.; Huete, A.R.; Kerr, Y.H.; Sorooshian, S. A modified soil adjusted vegetation index. *Remote Sens. Environ.* **1994**, *48*, 119–126. [CrossRef]
53. Tucker, C.J. Red and photographic infrared linear combinations for monitoring vegetation. *Remote Sens. Environ.* **1979**, *8*, 127–150. [CrossRef]
54. Gitelson, A.; Merzlyak, M.N. Spectral Reflectance Changes Associated with Autumn Senescence of *Aesculus hippocastanum* L. and *Acer platanoides* L. Leaves. Spectral Features and Relation to Chlorophyll Estimation. *J. Plant Physiol.* **1994**, *143*, 286–292. [CrossRef]
55. Baret, F.; Guyot, G. Potentials and limits of vegetation indices for LAI and APAR assessment. *Remote Sens. Environ.* **1991**, *35*, 161–173. [CrossRef]
56. Rouse, W.; Haas, R.H.; Deering, D.W. *Monitoring Vegetation Systems in the Great Plains with ERTS*; Third ERTS Symposium (NASA SP-351); NASA: Washington, DC, USA, 1974; Volume 1.
57. Agapiou, A.; Papadopoulos, N.; Sarris, A. Monitoring olive mills waste disposal areas in Crete using very high resolution satellite data. *Egypt. J. Remote Sens. Sp. Sci.* **2016**, *19*, 285–295. [CrossRef]
58. Cammalleri, C.; Ciraolo, G.; Minacapilli, M.; Rallo, G. Evapotranspiration from an Olive Orchard using Remote Sensing-Based Dual Crop Coefficient Approach. *Water Resour. Manag.* **2013**, *27*, 4877–4895. [CrossRef]
59. Diaz-Varela, R.A.; Zarco-Tejada, P.J.; Angileri, V.; Loudjani, P. Automatic identification of agricultural terraces through object-oriented analysis of very high resolution DSMs and multispectral imagery obtained from an unmanned aerial vehicle. *J. Environ. Manage.* **2014**, *134*, 117–126. [CrossRef]
60. Gertsis, A.; Vasilikiotis, C.; Zoukidis, K. Management zones delineation in olive grove using an unmanned aerial vehicle (UAV). *CEUR Workshop Proc.* **2015**, *1498*, 352–357.
61. Ghaderpour, E.; Ben Abbes, A.; Rhif, M.; Pagiatakis, S.D.; Farah, I.R. Non-stationary and unequally spaced NDVI time series analyses by the LSWAVE software. *Int. J. Remote Sens.* **2020**, *41*, 2374–2390. [CrossRef]
62. Karydas, C.G.; Sekuloska, T.; Silleos, G.N. Quantification and site-specification of the support practice factor when mapping soil erosion risk associated with olive plantations in the Mediterranean island of Crete. *Environ. Monit. Assess.* **2009**, *149*, 19–28. [CrossRef]
63. Kharrou, M.H.; Simonneaux, V.; Er-Raki, S.; Le Page, M.; Khabba, S.; Chehbouni, A. Assessing irrigation water use with remote sensing-based soil water balance at an irrigation scheme level in a semi-arid region of Morocco. *Remote Sens.* **2021**, *13*, 1133. [CrossRef]
64. Peña-Barragán, J.M.; Jurado-Expósito, M.; López-Granados, F.; Atenciano, S.; Sánchez-De La Orden, M.; García-Ferrer, A.; García-Torres, L. Assessing land-use in olive groves from aerial photographs. *Agric. Ecosyst. Environ.* **2004**, *103*, 117–122. [CrossRef]
65. Peña-Barragán, J.M.; López-Granados, F.; García-Torres, L.; Jurado-Expósito, M.; Sánchez de la Orden, M.; García-Ferrer, A. Discriminating cropping systems and agro-environmental measures by remote sensing. *Agron. Sustain. Dev.* **2008**, *28*, 355–362. [CrossRef]
66. Sepulcre-Cantó, G.; Zarco-Tejada, P.J.; Jiménez-Muñoz, J.C.; Sobrino, J.A.; De Miguel, E.; Villalobos, F.J. Detection of water stress in an olive orchard with thermal remote sensing imagery. *Agric. For. Meteorol.* **2006**, *136*, 31–44. [CrossRef]
67. Rondeaux, G.; Steven, M.; Baret, F. Optimization of soil-adjusted vegetation indices. *Remote Sens. Environ.* **1996**, *55*, 95–107. [CrossRef]
68. Roujean, J.L.; Breon, F.M. Estimating PAR absorbed by vegetation from bidirectional reflectance measurements. *Remote Sens. Environ.* **1995**, *51*, 375–384. [CrossRef]
69. Jordan, C.F. Derivation of Leaf-Area Index from Quality of Light on the Forest Floor. *Ecology* **1969**, *50*, 663–666. [CrossRef]
70. Huete, A.R. A soil-adjusted vegetation index (SAVI). *Remote Sens. Environ.* **1988**, *25*, 295–309. [CrossRef]
71. Carpintero, E.; Mateos, L.; Andreu, A.; González-Dugo, M.P. Effect of the differences in spectral response of Mediterranean tree canopies on the estimation of evapotranspiration using vegetation index-based crop coefficients. *Agric. Water Manag.* **2020**, *238*, 106201. [CrossRef]
72. Kaufman, Y.J.; Tanre, D. Atmospherically resistant vegetation index (ARVI) for EOS-MODIS. *IEEE Trans. Geosci. Remote Sens.* **1992**, *30*, 261–270. [CrossRef]

73. Broge, N.; Leblanc, E. Comparing prediction power and stability of broadband and hyperspectral vegetation indices for estimation of green leaf area index and canopy chlorophyll density. *Remote Sens. Environ.* **2001**, *76*, 156–172. [CrossRef]
74. Vogelmann, J.E.; Rock, B.N.; Moss, D.M. Red edge spectral measurements from sugar maple leaves. *Int. J. Remote Sens.* **1993**, *14*, 1563–1575. [CrossRef]
75. Thenkabail, P.S. *Remotely Sensed Data Characterization, Classification, and Accuracies—Remote Sensing Handbook Volume 1*, 1st ed.; Thenkabail, P.D., Ed.; CRC Press: Boca Raton, FL, USA, 2015; ISBN 9781482217872.
76. Belward, A.S.; Skøien, J.O. Who launched what, when and why; trends in global land-cover observation capacity from civilian earth observation satellites. *ISPRS J. Photogramm. Remote Sens.* **2015**, *103*, 115–128. [CrossRef]
77. Thenkabail, P.S. *Land Resources Monitoring, Modeling, and Mapping with Remote Sensing—Remote Ssensing Handbook Volume II*, 1st ed.; CRC Press: Boca Raton, FL, USA, 2015.
78. Mulla, D.J. Twenty five years of remote sensing in precision agriculture: Key advances and remaining knowledge gaps. *Biosyst. Eng.* **2013**, *114*, 358–371. [CrossRef]
79. What Are the Band Designations for the Landsat Satellites? Available online: https://www.usgs.gov/faqs/what-are-band-designations-landsat-satellites (accessed on 4 February 2022).
80. Lillesand, T.; Kiefer, R.W.; Chipman, J. *Remote Sensing and Image Interpretation*, 7th ed.; Wiley and Sons: New York, NY, USA, 2015; ISBN 978-1-118-91947-7.
81. Chaves, M.E.D.; Picoli, M.C.A.; Sanches, I.D. Recent applications of Landsat 8/OLI and Sentinel-2/MSI for land use and land cover mapping: A systematic review. *Remote Sens.* **2020**, *12*, 3062. [CrossRef]
82. De Bruin, S. Predicting the areal extent of land-cover types using classified imagery and geostatistics. *Remote Sens. Environ.* **2000**, *74*, 387–396. [CrossRef]
83. Efe, R.; Soykan, A.; Sönmez, S.; Cürebal, I. Quantifying the effect of landuse change on olive tree cultivation in the vicinity of Edremit between 1979 and 2006 using GIS and RS techniques. *Fresenius Environ. Bull.* **2008**, *17*, 696–704.
84. Kefi, M.; Pham, T.D.; Kashiwagi, K.; Yoshino, K. Identification of irrigated olive growing farms using remote sensing techniques. *Euro-Mediterr. J. Environ. Integr.* **2016**, *1*, 3. [CrossRef]
85. Tscheulin, T.; Neokosmidis, L.; Petanidou, T.; Settele, J. Influence of landscape context on the abundance and diversity of bees in Mediterranean olive groves. *Bull. Entomol. Res.* **2011**, *101*, 557–564. [CrossRef]
86. Chuvieco, E. *Fundamentals of Satellite Remote Sensing*, 2nd ed.; CRC Press: Boca Raton, FL, USA, 2016; ISBN 9781498728072.
87. Blum, M.; Lensky, I.M.; Nestel, D. Estimation of olive grove canopy temperature from MODIS thermal imagery is more accurate than interpolation from meteorological stations. *Agric. For. Meteorol.* **2013**, *176*, 90–93. [CrossRef]
88. Hoedjes, J.C.B.; Chehbouni, A.; Jacob, F.; Ezzahar, J.; Boulet, G. Deriving daily evapotranspiration from remotely sensed instantaneous evaporative fraction over olive orchard in semi-arid Morocco. *J. Hydrol.* **2008**, *354*, 53–64. [CrossRef]
89. Sishodia, R.P.; Ray, R.L.; Singh, S.K. Applications of remote sensing in precision agriculture: A review. *Remote Sens.* **2020**, *12*, 3136. [CrossRef]
90. *Campbell e Wynne Introduction to Remote Sensing*; The Guiford Press: New York, NY, USA, 2017; ISBN 9781609181765.
91. Li, Z.; Zhang, H.K.; Roy, D.P.; Yan, L.; Huang, H. Sharpening the Sentinel-2.10 and 20 m Bands to Planetscope-0.3 m Resolution. *Remote Sens.* **2020**, *12*, 2406. [CrossRef]
92. Masson, J.; Soille, P.; Mueller, R. Tests with VHR images for the identification of olive trees and other fruit trees in the European Union. *Proc. Remote Sens. Agric. Ecosyst. Hydrol. VI* **2004**, *5568*, 23–36. [CrossRef]
93. Karantzalos, K.G.; Argialas, D.P. Towards automatic olive tree extraction from satellite imagery. In *Geo-Imagery Bridging Continents. XXth ISPRS Congress*; Citeseer: Princeton, NJ, USA, 2004; pp. 12–23.
94. Nihal, C.; Ediz, U.; Masson, J. A Case Study of Developing An Olive Tree Database for Turkey. *Photogramm. Eng. Remote Sens.* **2009**, *75*, 1397–1405.
95. García Torres, L.; Peña-Barragán, J.M.; López-Granados, F.; Jurado-Expósito, M.; Fernández-Escobar, R. Automatic assessment of agro-environmental indicators from remotely sensed images of tree orchards and its evaluation using olive plantations. *Comput. Electron. Agric.* **2008**, *61*, 179–191. [CrossRef]
96. Iatrou, G.; Mourelatos, S.; Zartaloudis, Z.; Iatrou, M.; Gewehr, S.; Kalaitzopoulou, S. Remote sensing for the management of Verticillium wilt of olive. *Fresenius Environ. Bull.* **2016**, *25*, 3622–3628.
97. Solano, F.; Di Fazio, S.; Modica, G. A methodology based on GEOBIA and WorldView-3 imagery to derive vegetation indices at tree crown detail in olive orchards. *Int. J. Appl. Earth Obs. Geoinf.* **2019**, *83*, 101912. [CrossRef]
98. Lin, C.; Jin, Z.; Mulla, D.; Ghosh, R.; Guan, K.; Kumar, V.; Cai, Y. Toward large-scale mapping of tree crops with high-resolution satellite imagery and deep learning algorithms: A case study of olive orchards in Morocco. *Remote Sens.* **2021**, *13*, 1740. [CrossRef]
99. Abdelmoula, H.; Kallel, A.; Roujean, J.L.; Chaabouni, S.; Gargouri, K.; Ghrab, M.; Gastellu-Etchegorry, J.P.; Lauret, N. Olive biophysical property estimation based on Sentinel-2 image inversion. In Proceedings of the 2018 IEEE International Geoscience and Remote Sensing Symposium, Valencia, Spain, 22–27 July 2018; pp. 2869–2872. [CrossRef]
100. Houborg, R.; McCabe, M.F. High-Resolution NDVI from planet's constellation of earth observing nano-satellites: A new data source for precision agriculture. *Remote Sens.* **2016**, *8*, 768. [CrossRef]
101. Kopacz, J.R.; Herschitz, R.; Roney, J. Small satellites an overview and assessment. *Acta Astronaut.* **2020**, *170*, 93–105. [CrossRef]
102. Vizzari, M.; Santaga, F.; Benincasa, P. Sentinel 2-based nitrogen VRT fertilization in wheat: Comparison between traditional and simple precision practices. *Agronomy* **2019**, *9*, 278. [CrossRef]

103. Segarra, J.; Buchaillot, M.L.; Araus, J.L.; Kefauver, S.C. Remote sensing for precision agriculture: Sentinel-2 improved features and applications. *Agronomy* **2020**, *10*, 641. [CrossRef]
104. Martinis, S.; Caspard, M.; Plank, S.; Clandillon, S.; Haouet, S. Mapping burn scars, fire severity and soil erosion susceptibility in southern france using multisensoral satellite data. In Proceedings of the 2017 IEEE International Geoscience and Remote Sensing Symposium (IGARSS), Fort Worth, TX, USA, 23–28 July 2017; pp. 1099–1102.
105. De Luca, G.; Silva, J.M.N.; Modica, G. A workflow based on Sentinel-1 SAR data and open-source algorithms for unsupervised burned area detection in Mediterranean ecosystems. *GISci. Remote Sens.* **2021**, *58*, 516–541. [CrossRef]
106. Navrozidis, L.; Alexandridis, T.K.; Moshou, D.; Pantazi, X.E.; Alexandra Tamouridou, A.; Kozhukh, D.; Castef, F.; Lagopodi, A.; Zartaloudis, Z.; Mourelatos, S.; et al. Olive Trees Stress Detection Using Sentinel-2 Images. In Proceedings of the 2019 IEEE International Geoscience and Remote Sensing Symposium, Yokohama, Japan, 28 July–2 August 2019; pp. 7220–7223. [CrossRef]
107. Hornero, A.; Hernández-Clemente, R.; Beck, P.S.A.; Navas-Cortés, J.A.; Zarco-Tejada, P.J. Using sentinel-2 imagery to track changes produced by Xylella fastidiosa in olive trees. In Proceedings of the 2018 IEEE International Geoscience and Remote Sensing Symposium, Valencia, Spain, 22–27 July 2018; pp. 9060–9062. [CrossRef]
108. Hornero, A.; Hernández-Clemente, R.; North, P.R.J.; Beck, P.S.A.; Boscia, D.; Navas-Cortes, J.A.; Zarco-Tejada, P.J. Monitoring the incidence of Xylella fastidiosa infection in olive orchards using ground-based evaluations, airborne imaging spectroscopy and Sentinel-2 time series through 3-D radiative transfer modelling. *Remote Sens. Environ.* **2020**, *236*, 111480. [CrossRef]
109. Peters, J.; Van Coillie, F.; Westra, T.; De Wulf, R. Synergy of very high resolution optical and radar data for object-based olive grove mapping. *Int. J. Geogr. Inf. Sci.* **2011**, *25*, 971–989. [CrossRef]
110. Akcay, H.; Kaya, S.; Sertel, E.; Alganci, U. Determination of olive trees with multi-sensor data fusion. In Proceedings of the 2019 8th International Conference on Agro-Geoinformatics (Agro-Geoinformatics), Istanbul, Turkey, 16–19 July 2019; pp. 1–6. [CrossRef]
111. Molina, I.; Morillo, C.; García-Meléndez, E.; Guadalupe, R.; Roman, M.I. Characterizing olive grove canopies by Means of Ground-Based Hemispherical Photography and spaceborne RADAR data. *Sensors* **2011**, *11*, 7476–7501. [CrossRef]
112. Messina, G.; Modica, G. Applications of UAV thermal imagery in precision agriculture: State of the art and future research outlook. *Remote Sens.* **2020**, *12*, 1491. [CrossRef]
113. Nex, F.; Remondino, F. UAV for 3D mapping applications: A review. *Appl. Geomat.* **2014**, *6*, 1–15. [CrossRef]
114. Radoglou-Grammatikis, P.; Sarigiannidis, P.; Lagkas, T.; Moscholios, I. A compilation of UAV applications for precision agriculture. *Comput. Netw.* **2020**, *172*, 107148. [CrossRef]
115. Shakhatreh, H.; Sawalmeh, A.; Al-Fuqaha, A.; Dou, Z.; Almaita, E.; Khalil, I.; Othman, N.S.; Khreishah, A.; Guizani, M. Unmanned Aerial Vehicles: A Survey on Civil Applications and Key Research Challenges. *IEEE Access* **2018**, *7*, 48572–48634. [CrossRef]
116. De Luca, G.; Silva, J.M.N.; Cerasoli, S.; Araújo, J.; Campos, J.; Di Fazio, S.; Modica, G. Object-Based Land Cover Classification of Cork Oak Woodlands using UAV Imagery and Orfeo ToolBox. *Remote Sens.* **2019**, *11*, 1238. [CrossRef]
117. Pajares, G. Overview and Current Status of Remote Sensing Applications Based on Unmanned Aerial Vehicles (UAVs). *Photogramm. Eng. Remote Sens.* **2015**, *81*, 281–330. [CrossRef]
118. Yao, H.; Qin, R.; Chen, X. Unmanned Aerial Vehicle for Remote Sensing Applications—A Review. *Remote Sens.* **2019**, *11*, 1443. [CrossRef]
119. Tsouros, D.; Bibi, S.; Sarigiannidis, P.G. A review on UAV-based applications for precision agriculture. *Information* **2019**, *10*, 349. [CrossRef]
120. Khan, A.; Khan, U.; Waleed, M.; Khan, A.; Kamal, T.; Marwat, S.N.K.; Maqsood, M.; Aadil, F. Remote Sensing: An Automated Methodology for Olive Tree Detection and Counting in Satellite Images. *IEEE Access* **2018**, *6*, 77816–77828. [CrossRef]
121. Waleed, M.; Um, T.W.; Khan, A.; Ahmad, Z. An Automated Method for Detection and Enumeration of Olive Trees through Remote Sensing. *IEEE Access* **2020**, *8*, 108592–108601. [CrossRef]
122. Waleed, M.; Um, T.W.; Khan, A.; Khan, U. Automatic detection system of olive trees using improved K-means algorithm. *Remote Sens.* **2020**, *12*, 760. [CrossRef]
123. Torres-Sánchez, J.; López-Granados, F.; Serrano, N.; Arquero, O.; Peña, J.M. High-throughput 3-D monitoring of agricultural-tree plantations with Unmanned Aerial Vehicle (UAV) technology. *PLoS ONE* **2015**, *10*, e0130479. [CrossRef]
124. Torres-Sánchez, J.; López-Granados, F.; Borra-Serrano, I.; Peña, J.M. Assessing UAV-collected image overlap influence on computation time and digital surface model accuracy in olive orchards. *Precis. Agric.* **2018**, *19*, 115–133. [CrossRef]
125. Anifantis, A.S.; Camposeo, S.; Vivaldi, G.A.; Santoro, F.; Pascuzzi, S. Comparison of UAV photogrammetry and 3D modeling techniques with other currently used methods for estimation of the tree row volume of a super-high-density olive orchard. *Agriculture* **2019**, *9*, 233. [CrossRef]
126. Gómez-Gálvez, F.J.; Pérez-Mohedano, D.; de la Rosa-Navarro, R.; Belaj, A. High-throughput analysis of the canopy traits in the worldwide olive germplasm bank of Córdoba using very high-resolution imagery acquired from unmanned aerial vehicle (UAV). *Sci. Hortic.* **2020**, *278*, 109851. [CrossRef]
127. Stateras, D.; Kalivas, D. Assessment of olive tree canopy characteristics and yield forecast model using high resolution UAV imagery. *Agriculture* **2020**, *10*, 385. [CrossRef]
128. Zarco-Tejada, P.J.; Diaz-Varela, R.; Angileri, V.; Loudjani, P. Tree height quantification using very high resolution imagery acquired from an unmanned aerial vehicle (UAV) and automatic 3D photo-reconstruction methods. *Eur. J. Agron.* **2014**, *55*, 89–99. [CrossRef]

129. Di Nisio, A.; Adamo, F.; Acciani, G.; Attivissimo, F. Fast detection of olive trees affected by xylella fastidiosa from uavs using multispectral imaging. *Sensor* **2020**, *20*, 4915. [CrossRef]
130. Berni, J.; Zarco-Tejada, P.J.; Suarez, L.; Fereres, E. Thermal and Narrowband Multispectral Remote Sensing for Vegetation Monitoring From an Unmanned Aerial Vehicle. *IEEE Trans. Geosci. Remote Sens.* **2009**, *47*, 722–738. [CrossRef]
131. Jurado, J.M.; Ortega, L.; Cubillas, J.J.; Feito, F.R. Multispectral mapping on 3D models and multi-temporal monitoring for individual characterization of olive trees. *Remote Sens.* **2020**, *12*, 1106. [CrossRef]
132. Caruso, G.; Palai, G.; Marra, F.P.; Caruso, T. High-resolution UAV imagery for field olive (*Olea europaea* L.) phenotyping. *Horticulturae* **2021**, *7*, 258. [CrossRef]
133. Guillén-Climent, M.L.; Zarco-Tejada, P.J.; Villalobos, F.J. Estimating radiation interception in an olive orchard using physical models and multispectral airborne imagery. *Isr. J. Plant Sci.* **2012**, *60*, 107–121. [CrossRef]
134. Castrignanò, A.; Belmonte, A.; Antelmi, I.; Quarto, R.; Quarto, F.; Shaddad, S.; Sion, V.; Muolo, M.R.; Ranieri, N.A.; Gadaleta, G.; et al. Semi-automatic method for early detection of xylella fastidiosa in olive trees using uav multispectral imagery and geostatistical-discriminant analysis. *Remote Sens.* **2021**, *13*, 14. [CrossRef]
135. Castrignanò, A.; Belmonte, A.; Antelmi, I.; Quarto, R.; Quarto, F.; Shaddad, S.; Sion, V.; Muolo, M.R.; Ranieri, N.A.; Gadaleta, G.; et al. A geostatistical fusion approach using UAV data for probabilistic estimation of Xylella fastidiosa subsp. pauca infection in olive trees. *Sci. Total Environ.* **2021**, *752*, 141814. [CrossRef] [PubMed]
136. Jones, H.G.; Vaughan, R.A. *Remote Sensing of Vegetation Principles, Techniques, and Applications*; Oxford University Press: Oxford, UK, 2010; ISBN 9780199207794.
137. Avola, G.; Di Gennaro, S.F.; Cantini, C.; Riggi, E.; Muratore, F.; Tornambè, C.; Matese, A. Remotely sensed vegetation indices to discriminate field-grown olive cultivars. *Remote Sens.* **2019**, *11*, 1242. [CrossRef]
138. Modica, G.; Messina, G.; De Luca, G.; Fiozzo, V.; Praticò, S. Monitoring the vegetation vigor in heterogeneous citrus and olive orchards. A multiscale object-based approach to extract trees' crowns from UAV multispectral imagery. *Comput. Electron. Agric.* **2020**, *175*, 105500. [CrossRef]
139. Bellvert, J.; Zarco-Tejada, P.J.; Girona, J.; González-Dugo, V.; Fereres, E. A tool for detecting crop water status using airborne high-resolution thermal imagery. *WIT Trans. Ecol. Environ.* **2014**, *185*, 25–32. [CrossRef]
140. Berni, J.; Zarco-Tejada, P.J.; Sepulcre-Cantó, G.; Fereres, E.; Villalobos, F. Mapping canopy conductance and CWSI in olive orchards using high resolution thermal remote sensing imagery. *Remote Sens. Environ.* **2009**, *113*, 2380–2388. [CrossRef]
141. Egea, G.; Padilla-Díaz, C.M.; Martinez-Guanter, J.; Fernández, J.E.; Pérez-Ruiz, M. Assessing a crop water stress index derived from aerial thermal imaging and infrared thermometry in super-high density olive orchards. *Agric. Water Manag.* **2017**, *187*, 210–221. [CrossRef]
142. Poblete-Echeverría, C.; Ortega-Farías, S.; Lobos, G.A.; Romero, S.; Ahumada, L.; Escobar, A.; Fuentes, S. Non-invasive method to monitor plant water potential of an olive orchard using visible and near infrared spectroscopy analysis. *Acta Hortic.* **2014**, *1057*, 363–368. [CrossRef]
143. Riveros-Burgos, C.; Ortega-Farías, S.; Morales-Salinas, L.; Fuentes-Peñailillo, F.; Tian, F. Assessment of the clumped model to estimate olive orchard evapotranspiration using meteorological data and UAV-based thermal infrared imagery. *Irrig. Sci.* **2021**, *39*, 63–80. [CrossRef]
144. Calderón, R.; Navas-Cortés, J.A.; Lucena, C.; Zarco-Tejada, P.J. High-resolution airborne hyperspectral and thermal imagery for early detection of Verticillium wilt of olive using fluorescence, temperature and narrow-band spectral indices. *Remote Sens. Environ.* **2013**, *139*, 231–245. [CrossRef]
145. Calderón, R.; Navas-Cortés, J.; Zarco-Tejada, P. Early Detection and Quantification of Verticillium Wilt in Olive Using Hyperspectral and Thermal Imagery over Large Areas. *Remote Sens.* **2015**, *7*, 5584–5610. [CrossRef]
146. Thenkabail, P.S.; Lyon, J.G.; Huete, A. *Hyperspectral Remote Sensing of Vegetation VOL. 4 Advanced Applications in Remote Sensing of Agricultural Crops and Natural Vegetation*, 2nd ed.; CRC Press: Boca Raton, FL, USA, 2019.
147. Adão, T.; Hruška, J.; Pádua, L.; Bessa, J.; Peres, E.; Morais, R.; Sousa, J. Hyperspectral Imaging: A Review on UAV-Based Sensors, Data Processing and Applications for Agriculture and Forestry. *Remote Sens.* **2017**, *9*, 1110. [CrossRef]
148. Panday, U.S.; Pratihast, A.K.; Aryal, J.; Kayastha, R.B. A review on drone-based data solutions for cereal crops. *Drones* **2020**, *4*, 41. [CrossRef]
149. Rosell, J.R.; Llorens, J.; Sanz, R.; Arnó, J.; Ribes-Dasi, M.; Masip, J.; Escolà, A.; Camp, F.; Solanelles, F.; Gràcia, F.; et al. Obtaining the three-dimensional structure of tree orchards from remote 2D terrestrial LIDAR scanning. *Agric. For. Meteorol.* **2009**, *149*, 1505–1515. [CrossRef]
150. Rosell Polo, J.R.; Sanz, R.; Llorens, J.; Arnó, J.; Escolà, A.; Ribes-Dasi, M.; Masip, J.; Camp, F.; Gràcia, F.; Solanelles, F.; et al. A tractor-mounted scanning LIDAR for the non-destructive measurement of vegetative volume and surface area of tree-row plantations: A comparison with conventional destructive measurements. *Biosyst. Eng.* **2009**, *102*, 128–134. [CrossRef]
151. Dong, P.; Chen, Q. *LiDAR Remote Sensing and Applications*; CRC Press: Boca Raton, FL, USA; Taylor & Francis: Abingdon, UK, 2018; ISBN 9781351233354.
152. Rosell, J.R.; Sanz, R. A review of methods and applications of the geometric characterization of tree crops in agricultural activities. *Comput. Electron. Agric.* **2012**, *81*, 124–141. [CrossRef]
153. Lee, K.H.; Ehsani, R. A Laser Scanner Based Measurement System for Quantification of Citrus Tree Geometric Characteristics. *Appl. Eng. Agric.* **2009**, *25*, 777–788. [CrossRef]

154. Wallace, L.; Lucieer, A.; Watson, C.; Turner, D. Development of a UAV-LiDAR System with Application to Forest Inventory. *Remote Sens.* **2012**, *4*, 1519–1543. [CrossRef]
155. Barbera, G.; Cullotta, S. The Traditional Mediterranean Polycultural Landscape as Cultural Heritage: Its Origin and Historical Importance, Its Agro-Silvo-Pastoral Complexity and the Necessity for Its Identification and Inventory. In *Biocultural Diversity in Europe*; Springer: Berlin/Heidelberg, Germany, 2016; pp. 21–48.
156. Martínez, J.D.S.; Ruiz, A.O. The olive monoculture of Jaen: Historical structure, heritage values and cultural-touristic importance. *Cuad. Tur.* **2016**, *37*, 377–402. [CrossRef]
157. Cecchini, M.; Zambon, I.; Pontrandolfi, A.; Turco, R.; Colantoni, A.; Mavrakis, A.; Salvati, L. Urban sprawl and the 'olive' landscape: Sustainable land management for 'crisis' cities. *GeoJournal* **2019**, *84*, 237–255. [CrossRef]
158. Ponti, L.; Gutierrez, A.P.; Ruti, P.M.; Dell'Aquila, A. Fine-scale ecological and economic assessment of climate change on olive in the Mediterranean Basin reveals winners and losers. *Proc. Natl. Acad. Sci. USA* **2014**, *111*, 5598–5603. [CrossRef]
159. Brilli, L.; Chiesi, M.; Maselli, F.; Moriondo, M.; Gioli, B.; Toscano, P.; Zaldei, A.; Bindi, M. Simulation of olive grove gross primary production by the combination of ground and multi-sensor satellite data. *Int. J. Appl. Earth Obs. Geoinf.* **2013**, *23*, 29–36. [CrossRef]
160. Rallo, L.; Barranco, D.; Castro-García, S.; Connor, D.J.; del Campo, M.G.; Rallo, P. High-density olive plantations. *Hortic. Rev. (Am. Soc. Hortic. Sci.)* **2013**, *41*, 303–383. [CrossRef]
161. Scaramuzzi, F. Esproprio o Indennizzo per L'olivicoltura non Redditizia? Available online: https://www.georgofili.info/contenuti/esproprio-o-indennizzo-per-lolivicoltura-non-redditizia/487 (accessed on 2 February 2022).
162. Doygun, H. Effects of urban sprawl on agricultural land: A case study of Kahramanmaraş, Turkey. *Environ. Monit. Assess.* **2009**, *158*, 471–478. [CrossRef] [PubMed]
163. Lima, F.; Blanco-Sepúlveda, R.; Gómez-Moreno, M.L.; Dorado, J.; Peña, J.M. Mapping tillage direction and contour farming by object-based analysis of UAV images. *Comput. Electron. Agric.* **2021**, *187*, 106281. [CrossRef]
164. Tombesi, A.; Michelakis, N.; Pastor, M. Recommendations of the working group on olive farming production techniques and productivity. *Olivae* **1996**, *63*, 38–51.
165. International Olive Council. *Production Techniques in Olive Growing*, 1st ed.; International Olive Council: Madrid, Spain, 2007.
166. Gómez, J.; Infante-Amate, J.; de Molina, M.; Vanwalleghem, T.; Taguas, E.; Lorite, I. Olive Cultivation, its Impact on Soil Erosion and its Progression into Yield Impacts in Southern Spain in the Past as a Key to a Future of Increasing Climate Uncertainty. *Agriculture* **2014**, *4*, 170–198. [CrossRef]
167. Beaufoy, G. *The Environmental Impact of Olive Oil Production in the European Union: Practical Options for Improving the Environmental Impact*; European Commission: Brussels, Belgium, 2000; Volume 5210, p. 73.
168. Gómez, J.A. Sustainability using cover crops in mediterranean tree crops, olives and vines—Challenges and current knowledge. *Hung. Geogr. Bull.* **2017**, *66*, 13–28. [CrossRef]
169. Gómez, J.A.; Campos, M.; Guzmán, G.; Castillo-Llanque, F.; Vanwalleghem, T.; Lora, Á.; Giráldez, J.V. Soil erosion control, plant diversity, and arthropod communities under heterogeneous cover crops in an olive orchard. *Environ. Sci. Pollut. Res.* **2018**, *25*, 977–989. [CrossRef]
170. Palese, A.M.; Vignozzi, N.; Celano, G.; Agnelli, A.E.; Pagliai, M.; Xiloyannis, C. Influence of soil management on soil physical characteristics and water storage in a mature rainfed olive orchard. *Soil Tillage Res.* **2014**, *144*, 96–109. [CrossRef]
171. Bombino, G.; Denisi, P.; Gómez, J.A.; Zema, D.A. Water infiltration and surface runoff in steep clayey soils of olive groves under different management practices. *Water* **2019**, *11*, 240. [CrossRef]
172. Gómez, J.A.; Sobrinho, T.A.; Giráldez, J.V.; Fereres, E. Soil management effects on runoff, erosion and soil properties in an olive grove of Southern Spain. *Soil Tillage Res.* **2009**, *102*, 5–13. [CrossRef]
173. López-Vicente, M.; García-Ruiz, R.; Guzmán, G.; Vicente-Vicente, J.L.; Van Wesemael, B.; Gómez, J.A. Temporal stability and patterns of runoff and runon with different cover crops in an olive orchard (SW Andalusia, Spain). *Catena* **2016**, *147*, 125–137. [CrossRef]
174. Gómez, J.A.; Llewellyn, C.; Basch, G.; Sutton, P.B.; Dyson, J.S.; Jones, C.A. The effects of cover crops and conventional tillage on soil and runoff loss in vineyards and olive groves in several Mediterranean countries. *Soil Use Manag.* **2011**, *27*, 502–514. [CrossRef]
175. Moreno, B.; Garcia-Rodriguez, S.; Cañizares, R.; Castro, J.; Benítez, E. Rainfed olive farming in south-eastern Spain: Long-term effect of soil management on biological indicators of soil quality. *Agric. Ecosyst. Environ.* **2009**, *131*, 333–339. [CrossRef]
176. Morgan, R.P.C. *Soil Erosion & Conservation*; Wiley & Sons: Hoboken, NJ, USA, 2005; Volume 53, ISBN 9788578110796.
177. Pereira, H.M.; Domingos, T.; Vicente, L. Assessing ecosystem services at different scales in the Portugal Millennium Ecosystem Assessment. In *Millennium Ecosystem Assessment, Bridging Scales and Epistemologies*; Reid, W.V., Berkes, F., Wilbanks, T., Capistrano, D., Eds.; Island Press: Washington, DC, USA, 2006; pp. 59–79.
178. Dunjó, G.; Pardini, G.; Gispert, M. Land use change effects on abandoned terraced soils in a Mediterranean catchment, NE Spain. *CATENA* **2003**, *52*, 23–37. [CrossRef]
179. Martínez-Casasnovas, J.A.; Ramos, M.C.; Cots-Folch, R. Influence of the EU CAP on terrain morphology and vineyard cultivation in the Priorat region of NE Spain. *Land Use Policy* **2010**, *27*, 11–21. [CrossRef]
180. Modica, G.; Praticò, S.; Di Fazio, S. Abandonment of traditional terraced landscape: A change detection approach (a case study in Costa Viola, Calabria, Italy). *L. Degrad. Dev.* **2017**, *28*, 2608–2622. [CrossRef]

181. Fernández, T.; Pérez, J.L.; Cardenal, J.; Gómez, J.M.; Colomo, C.; Delgado, J. Analysis of landslide evolution affecting olive groves using UAV and photogrammetric techniques. *Remote Sens.* **2016**, *8*, 837. [CrossRef]
182. Fleskens, L. A typology of sloping and mountainous olive plantation systems to address natural resources management. *Ann. Appl. Biol.* **2008**, *153*, 283–297. [CrossRef]
183. Domazetovic, F.; Šiljeg, A.; Maric, I.; Jurišic, M. Assessing the vertical accuracy of worldview-3 stereo-extracted digital surface model over olive groves. In Proceedings of the GISTAM 2020—6th International Conference on Geographical Information Systems Theory, Applications and Management, Prague, Czech Republic, 7–9 May 2020; pp. 246–253. [CrossRef]
184. Beniaich, A.; Silva, M.L.N.; Guimarães, D.V.; Bispo, D.F.A.; Avanzi, J.C.; Curi, N.; Pio, R.; Dondeyne, S. Assessment of soil erosion in olive orchards (*Olea europaea* L.) Under cover crops management systems in the tropical region of Brazil. *Rev. Bras. Cienc. Do Solo* **2020**, *44*, e0190088. [CrossRef]
185. Rodriguez-Galiano, V.F.; Ghimire, B.; Rogan, J.; Chica-olmo, M.; Rigol-sanchez, J.P. An assessment of the effectiveness of a random forest classifier for land-cover classification. *ISPRS J. Photogramm. Remote Sens.* **2012**, *67*, 93–104. [CrossRef]
186. Anderson, J.; Hardy, E.E.; Roach, J.T.; Witmer, R.E. *A Land Use and Land Cover Classification System for Use with Remote Sensor Data*; Professional Paper; US Government Printing Office: Washington, DC, USA, 1976.
187. Pereira, P.; Brevik, E.C.; Muñoz-Rojas, M.; Miller, B.A.; Smetanova, A.; Depellegrin, D.; Misiune, I.; Novara, A.; Cerdà, A. Soil Mapping and Processes Modeling for Sustainable Land Management. In *Soil Mapping and Process Modeling for Sustainable Land Use Management*; Elsevier: Amsterdam, The Netherlands, 2017; pp. 29–60.
188. Metternicht, G. *Land Use and Spatial Planning: Enabling Sustainable Management of Land Resources*; SpringerBriefs in Earth Sciences; Springer International Publishing: Cham, Switzerlan, 2018; ISBN 978-3-319-71860-6.
189. Ciriza, R.; Sola, I.; Albizua, L.; álvarez-Mozos, J.; González-Audícana, M. Automatic detection of uprooted orchards based on orthophoto texture analysis. *Remote Sens.* **2017**, *9*, 492. [CrossRef]
190. Birth, G.S.; McVey, G.R. Measuring the Color of Growing Turf with a Reflectance Spectrophotometer 1. *Agron. J.* **1968**, *60*, 640–643. [CrossRef]
191. Weissteiner, C.J.; Strobl, P.; Sommer, S. Assessment of status and trends of olive farming intensity in EU-Mediterranean countries using remote sensing time series and land cover data. *Ecol. Indic.* **2011**, *11*, 601–610. [CrossRef]
192. Deardorff, J.W. Efficient prediction of ground surface temperature and moisture, with inclusion of a layer of vegetation. *J. Geophys. Res.* **1978**, *83*, 1889. [CrossRef]
193. Torkashvand, A.M.; Shadparvar, V. Proposing a methodology in preparation of olive orchards map by remote sensing and geographic information system. *J. Med. Plants Res.* **2012**, *6*, 680–688. [CrossRef]
194. Ghaderpour, E.; Pagiatakis, S.D. Least-Squares Wavelet Analysis of Unequally Spaced and Non-stationary Time Series and Its Applications. *Math. Geosci.* **2017**, *49*, 819–844. [CrossRef]
195. Dermeche, S.; Nadour, M.; Larroche, C.; Moulti-Mati, F.; Michaud, P. Olive mill wastes: Biochemical characterizations and valorization strategies. *Process Biochem.* **2013**, *48*, 1532–1552. [CrossRef]
196. Roig, A.; Cayuela, M.L.; Sánchez-Monedero, M.A. An overview on olive mill wastes and their valorisation methods. *Waste Manag.* **2006**, *26*, 960–969. [CrossRef]
197. Borja, R.; Sánchez, E.; Raposo, F.; Rincón, B.; Jiménez, A.M.; Martín, A. A study of the natural biodegradation of two-phase olive mill solid waste during its storage in an evaporation pond. *Waste Manag.* **2006**, *26*, 477–486. [CrossRef]
198. Raposo, F.; Borja, R.; Sánchez, E.; Martín, M.A.; Martín, A. Performance and kinetic evaluation of the anaerobic digestion of two-phase olive mill effluents in reactors with suspended and immobilized biomass. *Water Res.* **2004**, *38*, 2017–2026. [CrossRef]
199. Davies, L.C.; Vilhena, A.M.; Novais, J.M.; Martins-Dias, S. Olive mill wastewater characteristics: Modelling and statistical analysis. *Grasas Y Aceites* **2004**, *55*, 233–241. [CrossRef]
200. El-Abbassi, A.; Saadaoui, N.; Kiai, H.; Raiti, J.; Hafidi, A. Potential applications of olive mill wastewater as biopesticide for crops protection. *Sci. Total Environ.* **2017**, *576*, 10–21. [CrossRef]
201. Paredes, C.; Cegarra, J.; Roig, A.; Sánchez-Monedero, M.A.; Bernal, M.P. Characterization of olive mill wastewater (alpechin) and its sludge for agricultural purposes. *Bioresour. Technol.* **1999**, *67*, 111–115. [CrossRef]
202. Rincon, B.; Fermoso, F.G.; Borj, R. Olive Oil Mill Waste Treatment:Improving the Sustainability of the Olive Oil Industry with Anaerobic Digestion Technology. In *Olive Oil—Constituents, Quality, Health Properties and Bioconversions*; InTech: London, UK, 2012.
203. Azbar, N.; Bayram, A.; Filibeli, A.; Muezzinoglu, A.; Sengul, F.; Ozer, A. A Review of Waste Management Options in Olive Oil Production. *Crit. Rev. Environ. Sci. Technol.* **2004**, *34*, 209–247. [CrossRef]
204. Benalia, S.; Falcone, G.; Stillitano, T.; De Luca, A.I.; Strano, A.; Gulisano, G.; Zimbalatti, G.; Bernardi, B. Increasing the Content of Olive Mill Wastewater in Biogas Reactors for a Sustainable Recovery: Methane Productivity and Life Cycle Analyses of the Process. *Foods* **2021**, *10*, 1029. [CrossRef]
205. Hanifi, S.; Hadrami, I. El Olive Mill Wastewaters: Diversity of the Fatal Product in Olive Oil Industry and its Valorisation as Agronomical Amendment of Poor Soils: A Review. *J. Agron.* **2008**, *8*, 1–13. [CrossRef]
206. Niaounakis, M.; Halvadakis, C.P. *Olive Processing Waste Management. Literature Review and Patent Survey*; Te Management Series; Elsevier Ltd.: Amsterdam, The Netherlands, 2006; Volume 5.
207. Tsagaraki, E.; Lazarides, H.N.; Petrotos, K.B. Olive Mill Wastewater Treatment. In *Utilization of By-Products and Treatment of Waste in the Food Industry*; Springer: New York City, NY, USA, 2007; pp. 133–157.

208. Doula, M.K.; Kavvadias, V.; Elaiopoulos, K. Proposed soil indicators for olive mill waste (OMW) disposal areas. *Water. Air. Soil Pollut.* **2013**, *224*, 1621. [CrossRef]
209. Asfi, M.; Ouzounidou, G.; Panajiotidis, S.; Therios, I.; Moustakas, M. Toxicity effects of olive-mill wastewater on growth, photosynthesis and pollen morphology of spinach plants. *Ecotoxicol. Environ. Saf.* **2012**, *80*, 69–75. [CrossRef]
210. Barbera, A.C.; Maucieri, C.; Cavallaro, V.; Ioppolo, A.; Spagna, G. Effects of spreading olive mill wastewater on soil properties and crops, a review. *Agric. Water Manag.* **2013**, *119*, 43–53. [CrossRef]
211. Doula, M.K.; Tinivella, F.; Ortego, L.L.M.; Kavvadias, V.A.; Sarris, A.; Theocharopoulos, S.; Sanchez-Monedero, M.A.; Elaiopouls, K. Good Practices for the Agronomic Use of Olive Mill Wastes—Application Guide (PROSODOL); edited by M.K Doula, LIFE07/ENV/GR/000280; 2012. Available online: https://www.researchgate.net/publication/298786494_Good_Practices_for_the_Agronomic_Use_of_Olive_Mill_Wastes (accessed on 2 October 2022).
212. Mekki, A.; Dhouib, A.; Sayadi, S. Evolution of several soil properties following amendment with olive mill wastewater. *Prog. Nat. Sci.* **2009**, *19*, 1515–1521. [CrossRef]
213. Rinaldi, M.; Rana, G.; Introna, M. Olive-mill wastewater spreading in southern Italy: Effects on a durum wheat crop. *F. Crop. Res.* **2003**, *84*, 319–326. [CrossRef]
214. Di Bene, C.; Pellegrino, E.; Debolini, M.; Silvestri, N.; Bonari, E. Short- and long-term effects of olive mill wastewater land spreading on soil chemical and biological properties. *Soil Biol. Biochem.* **2013**, *56*, 21–30. [CrossRef]
215. Koutsos, T.M.; Chatzistathis, T.; Balampekou, E.I. A new framework proposal, towards a common EU agricultural policy, with the best sustainable practices for the re-use of olive mill wastewater. *Sci. Total Environ.* **2018**, *622–623*, 942–953. [CrossRef]
216. Gao, B. NDWI—A normalized difference water index for remote sensing of vegetation liquid water from space. *Remote Sens. Environ.* **1996**, *58*, 257–266. [CrossRef]
217. Karydas, C.G.; Sarakiotis, I.L.; Zalidis, G.C. Multi-scale risk assessment of stream pollution by wastewater of olive oil mills in Kolymvari, Crete. *Earth Sci. Inform.* **2014**, *7*, 47–58. [CrossRef]
218. Elhag, M.; Bahrawi, J.A.; Galal, H.K.; Aldhebiani, A.; Al-Ghamdi, A.A.M. Stream network pollution by olive oil wastewater risk assessment in Crete, Greece. *Environ. Earth Sci.* **2017**, *76*, 278. [CrossRef]
219. Xiloyannis, C.; Dichio, B.; Nuzzo, V.; Celano, G. Defence strategies of olive against water stress. *Acta Hortic.* **1999**, *474*, 423–426. [CrossRef]
220. Gucci, R.; Lodolini, E.; Rapoport, H.F. Productivity of olive trees with different water status and crop load. *J. Hortic. Sci. Biotechnol.* **2007**, *82*, 648–656. [CrossRef]
221. Moriondo, M.; Ferrise, R.; Trombi, G.; Brilli, L.; Dibari, C.; Bindi, M. Modelling olive trees and grapevines in a changing climate. *Environ. Model. Softw.* **2015**, *72*, 387–401. [CrossRef]
222. Marino, G.; Pallozzi, E.; Cocozza, C.; Tognetti, R.; Giovannelli, A.; Cantini, C.; Centritto, M. Assessing gas exchange, sap flow and water relations using tree canopy spectral reflectance indices in irrigated and rainfed *Olea europaea* L. *Environ. Exp. Bot.* **2014**, *99*, 43–52. [CrossRef]
223. Fraga, H.; Moriondo, M.; Leolini, L.; Santos, J.A. Mediterranean Olive Orchards under Climate Change: A Review of Future Impacts and Adaptation Strategies. *Agronomy* **2020**, *11*, 56. [CrossRef]
224. Zipori, I.; Erel, R.; Yermiyahu, U.; Ben-Gal, A.; Dag, A. Sustainable management of olive orchard nutrition: A review. *Agriculture* **2020**, *10*, 11. [CrossRef]
225. Arampatzis, G.; Hatzigiannakis, E.; Pisinaras, V.; Kourgialas, N.; Psarras, G.; Kinigopoulou, V.; Panagopoulos, A.; Koubouris, G. Soil water content and olive tree yield responses to soil management, irrigation, and precipitation in a hilly Mediterranean area. *J. Water Clim. Chang.* **2018**, *9*, 672–678. [CrossRef]
226. Proietti, P.; Antognozzi, E. Effect of irrigation on fruit quality of table olives (*Olea europaea*), cultivar 'Ascolana tenera. *New Zeal. J. Crop Hortic. Sci.* **1996**, *24*, 175–181. [CrossRef]
227. Inglese, P.; Barone, E.; Gullo, G. The effect of complementary irrigation on fruit growth, ripening pattern and oil characteristics of olive (*Olea europaea* L.) cv. Carolea. *J. Hortic. Sci. Biotechnol.* **1996**, *71*, 257–263. [CrossRef]
228. Goldhamer, D.A.; Dunai, J.; Ferguson, L.F. Irrigation requirements of olive trees and responses to sustained deficit irrigation. *Acta Hortic.* **1994**, *356*, 172–175. [CrossRef]
229. Ben-Gal, A.; Agam, N.; Alchanatis, V.; Cohen, Y.; Yermiyahu, U.; Zipori, I.; Presnov, E.; Sprintsin, M.; Dag, A. Evaluating water stress in irrigated olives: Correlation of soil water status, tree water status, and thermal imagery. *Irrig. Sci.* **2009**, *27*, 367–376. [CrossRef]
230. Padilla-Díaz, C.M.; Rodriguez-Dominguez, C.M.; Hernandez-Santana, V.; Perez-Martin, A.; Fernández, J.E. Scheduling regulated deficit irrigation in a hedgerow olive orchard from leaf turgor pressure related measurements. *Agric. Water Manag.* **2016**, *164*, 28–37. [CrossRef]
231. Fernández, J.E. Plant-based sensing to monitor water stress: Applicability to commercial orchards. *Agric. Water Manag.* **2014**, *142*, 99–109. [CrossRef]
232. Santos-Rufo, A.; Mesas-Carrascosa, F.J.; García-Ferrer, A.; Meroño-Larriva, J.E. Wavelength selection method based on partial least square from hyperspectral unmanned aerial vehicle orthomosaic of irrigated olive orchards. *Remote Sens.* **2020**, *12*, 3426. [CrossRef]
233. Molden, D.; Murray-Rust, H.; Sakthivadivel, R.; Makin, I. A water-productivity framework for understanding and action. In *Water Productivity in Agriculture: Limits and Opportunities for Improvement*; CABI: Wallingford, UK, 2003; pp. 1–18.

234. Pereira, L.S.; Cordery, I.; Iacovides, I. Improved indicators of water use performance and productivity for sustainable water conservation and saving. *Agric. Water Manag.* **2012**, *108*, 39–51. [CrossRef]
235. Fernández, J.E.; Diaz-Espejo, A.; Romero, R.; Hernandez-Santana, V.; García, J.M.; Padilla-Díaz, C.M.; Cuevas, M.V. *Precision Irrigation in Olive (Olea europaea L.) Tree Orchards*; Elsevier Inc.: Amsterdam, The Netherlands, 2018; ISBN 9780128131640.
236. Tognetti, R.; Morales-Sillero, A.; D'Andria, R.; Fernández, J.E.; Lavini, A.; Sebastiani, L.; Troncoso, A. Deficit irrigation and fertigation practices in olive growing: Convergences and divergences in two case studies. *Plant Biosyst.* **2008**, *142*, 138–148. [CrossRef]
237. Gucci, R.; Caruso, G.; Gennai, C.; Esposto, S.; Urbani, S.; Servili, M. Fruit growth, yield and oil quality changes induced by deficit irrigation at different stages of olive fruit development. *Agric. Water Manag.* **2019**, *212*, 88–98. [CrossRef]
238. Gucci, R.; Caruso, G. Environmental stresses and sustainable olive growing. *Acta Hortic.* **2011**, *924*, 19–30. [CrossRef]
239. Fernández, J.E. Plant-based methods for irrigation scheduling of woody crops. *Horticulturae* **2017**, *3*, 35. [CrossRef]
240. Smith, R.J.; Baillie, J.N. Defining Precision Irrigation: A New Approach to Irrigation Management. In Proceedings of the Irrigation Australia 2009: Irrigation Australia Irrigation and Drainage Conference, Swan Hill, Australia, 18–21 October 2009.
241. Gonzalez-Dugo, V.; Zarco-Tejada, P.; Nicolás, E.; Nortes, P.A.; Alarcón, J.J.; Intrigliolo, D.S.; Fereres, E. Using high resolution UAV thermal imagery to assess the variability in the water status of five fruit tree species within a commercial orchard. *Precis. Agric.* **2013**, *14*, 660–678. [CrossRef]
242. Cohen, Y.; Alchanatis, V.; Saranga, Y.; Rosenberg, O.; Sela, E.; Bosak, A. Mapping water status based on aerial thermal imagery: Comparison of methodologies for upscaling from a single leaf to commercial fields. *Precis. Agric.* **2017**, *18*, 801–822. [CrossRef]
243. Gerhards, M.; Schlerf, M.; Mallick, K.; Udelhoven, T. Challenges and future perspectives of multi-/Hyperspectral thermal infrared remote sensing for crop water-stress detection: A review. *Remote Sens.* **2019**, *11*, 1240. [CrossRef]
244. Khanal, S.; Fulton, J.; Shearer, S. An overview of current and potential applications of thermal remote sensing in precision agriculture. *Comput. Electron. Agric.* **2017**, *139*, 22–32. [CrossRef]
245. Gago, J.; Douthe, C.; Coopman, R.E.; Gallego, P.P.; Ribas-Carbo, M.; Flexas, J.; Escalona, J.; Medrano, H. UAVs challenge to assess water stress for sustainable agriculture. *Agric. Water Manag.* **2015**, *153*, 9–19. [CrossRef]
246. Jackson, R.D.; Idso, S.B.; Reginato, R.J.; Pinter, J.P.J. Canopy temperature as a crop water stress indicator. *Water Resour. Res.* **1981**, *17*, 1133–1138. [CrossRef]
247. Lapidot, O.; Ignat, T.; Rud, R.; Rog, I.; Alchanatis, V.; Klein, T. Use of thermal imaging to detect evaporative cooling in coniferous and broadleaved tree species of the Mediterranean maquis. *Agric. For. Meteorol.* **2019**, *271*, 285–294. [CrossRef]
248. Hsiao, T.C. Plants response to water stress. *Ann Rev. Plant Physiol.* **1973**, *24*, 519–570. [CrossRef]
249. Er-Raki, S.; Chehbouni, A.; Hoedjes, J.; Ezzahar, J.; Duchemin, B.; Jacob, F. Improvement of FAO-56 method for olive orchards through sequential assimilation of thermal infrared-based estimates of ET. *Agric. Water Manag.* **2008**, *95*, 309–321. [CrossRef]
250. Ramírez-Cuesta, J.M.; Allen, R.G.; Zarco-Tejada, P.J.; Kilic, A.; Santos, C.; Lorite, I.J. Impact of the spatial resolution on the energy balance components on an open-canopy olive orchard. *Int. J. Appl. Earth Obs. Geoinf.* **2019**, *74*, 88–102. [CrossRef]
251. Ortega-Farías, S.; Ortega-Salazar, S.; Poblete, T.; Kilic, A.; Allen, R.; Poblete-Echeverría, C.; Ahumada-Orellana, L.; Zuñiga, M.; Sepúlveda, D. Estimation of Energy Balance Components over a Drip-Irrigated Olive Orchard Using Thermal and Multispectral Cameras Placed on a Helicopter-Based Unmanned Aerial Vehicle (UAV). *Remote Sens.* **2016**, *8*, 638. [CrossRef]
252. Sobrino, J.A.; Jiménez-Muñoz, J.C.; Zarco-Tejada, P.J.; Sepulcre-Cantó, G.; de Miguel, E. Land surface temperature derived from airborne hyperspectral scanner thermal infrared data. *Remote Sens. Environ.* **2006**, *102*, 99–115. [CrossRef]
253. Gillespie, A.; Rokugawa, S.; Matsunaga, T.; Steven Cothern, J.; Hook, S.; Kahle, A.B. A temperature and emissivity separation algorithm for advanced spaceborne thermal emission and reflection radiometer (ASTER) images. *IEEE Trans. Geosci. Remote Sens.* **1998**, *36*, 1113–1126. [CrossRef]
254. Castelli, G.; Oliveira, L.A.A.; Abdelli, F.; Dhaou, H.; Bresci, E.; Ouessar, M. Effect of traditional check dams (jessour) on soil and olive trees water status in Tunisia. *Sci. Total Environ.* **2019**, *690*, 226–236. [CrossRef]
255. Hardisky, M.A.; Klemas, V.; Smart, R.M. The influence of soil salinity, growth form, and leaf moisture on the spectral radiance of Spartina alterniflora canopies. *Photogramm. Eng. Remote Sens.* **1983**, *49*, 77–83.
256. Sriwongsitanon, N.; Gao, H.; Savenije, H.H.G.; Maekan, E.; Saengsawang, S.; Thianpopirug, S. Comparing the Normalized Difference Infrared Index (NDII) with root zone storage in a lumped conceptual model. *Hydrol. Earth Syst. Sci.* **2016**, *20*, 3361–3377. [CrossRef]
257. Poblete-Echeverría, C.; Sepulveda-Reyes, D.; Ortega-Farias, S.; Zuñiga, M.; Fuentes, S. Plant water stress detection based on aerial and terrestrial infrared thermography: A study case from vineyard and olive orchard. *Acta Hortic.* **2016**, *1112*, 141–146. [CrossRef]
258. Marques, P.; Padua, L.; Brito, T.; Sousa, J.J.; Fernandes-Silva, A. Monitoring of Olive Trees Temperatures under Different Irrigation Strategies by UAV Thermal Infrared Imagery. In Proceedings of the IGARSS 2020—2020 IEEE International Geoscience and Remote Sensing Symposium, Waikoloa, HI, USA, 26 September–2 October 2020; pp. 4550–4553.
259. Testi, L.; Goldhamer, D.A.; Iniesta, F.; Salinas, M. Crop water stress index is a sensitive water stress indicator in pistachio trees. *Irrig. Sci.* **2008**, *26*, 395–405. [CrossRef]
260. Bellvert, J.; Zarco-Tejada, P.J.; Girona, J.; Fereres, E. Mapping crop water stress index in a 'Pinot-noir' vineyard: Comparing ground measurements with thermal remote sensing imagery from an unmanned aerial vehicle. *Precis. Agric.* **2014**, *15*, 361–376. [CrossRef]

261. Martín-Vertedor, A.I.; Rodríguez, J.M.P.; Losada, H.P.; Castiel, E.F. Interactive responses to water deficits and crop load in olive (*Olea europaea* L., cv. Morisca). II: Water use, fruit and oil yield. *Agric. Water Manag.* **2011**, *98*, 950–958. [CrossRef]
262. Jones, C.; Weckler, P.; Maness, N.; Stone, M.; Jayasekara, R. Estimating Water Stress in Plants Using Hyperspectral Sensing. In Proceedings of the 2004, Ottawa, ON, Canada, 1–4 August 2004; American Society of Agricultural and Biological Engineers: St. Joseph, MI, USA, 2004.
263. Fuentes, S.; De Bei, R.; Pech, J.; Tyerman, S. Computational water stress indices obtained from thermal image analysis of grapevine canopies. *Irrig. Sci.* **2012**, *30*, 523–536. [CrossRef]
264. Brenner, A.J.; Incoll, L.D. The effect of clumping and stomatal response on evaporation from sparsely vegetated shrublands. *Agric. For. Meteorol.* **1997**, *84*, 187–205. [CrossRef]
265. Barnes, E.M.; Clarke, T.R.; Richards, S.E.; Colaizzi, P.D.; Haberland, J.; Kostrzewski, M.; Waller, P.; Choi, C.; Riley, E.; Thompson, T.; et al. Coincident detection of crop water stress, nitrogen status and canopy density using ground based multispectral data. In Proceedings of the 5th International Conference on Precision Agriculture and Other Resource Management, Bloomington, MN, USA, 16–19 July 2000.
266. Fordellone, M.; Bellincontro, A.; Mencarelli, F. Partial least squares discriminant analysis: A dimensionality reduction method to classify hyperspectral data. *Stat. Appl.* **2019**, *31*, 181–200. [CrossRef]
267. Krishnan, A.; Williams, L.J.; McIntosh, A.R.; Abdi, H. Partial Least Squares (PLS) methods for neuroimaging: A tutorial and review. *Neuroimage* **2011**, *56*, 455–475. [CrossRef]
268. Barbedo, J.G.A. A review on the use of unmanned aerial vehicles and imaging sensors for monitoring and assessing plant stresses. *Drones* **2019**, *3*, 40. [CrossRef]
269. Nolè, G. Remote Sensing Techniques in Olive-Growing: A Review. *Curr. Investig. Agric. Curr. Res.* **2018**, *2*, 205–208. [CrossRef]
270. Yang, C. High resolution satellite imaging sensors for precision agriculture. *Front. Agric. Sci. Eng.* **2018**, *5*, 393–405. [CrossRef]
271. Zhu, X.; Cai, F.; Tian, J.; Williams, T.K.A. Spatiotemporal fusion of multisource remote sensing data: Literature survey, taxonomy, principles, applications, and future directions. *Remote Sens.* **2018**, *10*, 527. [CrossRef]
272. Sozzi, M.; Marinello, F.; Pezzuolo, A.; Sartori, L. Benchmark of Satellites Image Services for Precision Agricultural use. In Proceedings of the AgEng Conference, Wageningen, The Netherlands, 8–12 July 2018.
273. Gao, F.; Masek, J.; Schwaller, M.; Hall, F. On the blending of the Landsat and MODIS surface reflectance: Predicting daily Landsat surface reflectance. *IEEE Trans. Geosci. Remote Sens.* **2006**, *44*, 2207–2218. [CrossRef]
274. Manfreda, S.; McCabe, M.F.; Miller, P.E.; Lucas, R.; Madrigal, V.P.; Mallinis, G.; Ben Dor, E.; Helman, D.; Estes, L.; Ciraolo, G.; et al. On the use of unmanned aerial systems for environmental monitoring. *Remote Sens.* **2018**, *10*, 641. [CrossRef]
275. Zhang, C.; Kovacs, J.M. The application of small unmanned aerial systems for precision agriculture: A review. *Precis. Agric.* **2012**, *13*, 693–712. [CrossRef]
276. Näsi, R.; Honkavaara, E.; Lyytikäinen-Saarenmaa, P.; Blomqvist, M.; Litkey, P.; Hakala, T.; Viljanen, N.; Kantola, T.; Tanhuanpää, T.; Holopainen, M. Using UAV-Based Photogrammetry and Hyperspectral Imaging for Mapping Bark Beetle Damage at Tree-Level. *Remote Sens.* **2015**, *7*, 15467–15493. [CrossRef]
277. Di Fazio, S.; Modica, G. Historic rural landscapes: Sustainable planning strategies and action criteria. The Italian experience in the Global and European Context. *Sustainability* **2018**, *10*, 3834. [CrossRef]
278. Hernández-Mogollón, J.M.; Di-Clemente, E.; Folgado-Fernández, J.A.; Campón-Cerro, A.M. Olive oil tourism: State of the art. *Tour. Hosp. Manag.* **2019**, *25*, 179–207. [CrossRef]
279. DeFries, R.; Rosenzweig, C. Toward a whole-landscape approach for sustainable land use in the tropics. *Proc. Natl. Acad. Sci. USA* **2010**, *107*, 19627–19632. [CrossRef] [PubMed]
280. Verburg, P.H.; Mertz, O.; Erb, K.-H.; Haberl, H.; Wu, W. Land system change and food security: Towards multi-scale land system solutions. *Curr. Opin. Environ. Sustain.* **2013**, *5*, 494–502. [CrossRef] [PubMed]
281. ISPAG. ISPAG Precision Agriculture Definition. 2019. Available online: https://www.springer.com/journal/11119/updates/17240272 (accessed on 2 October 2022).